5

Biomechanics of Locomotion in Sharks, Rays, and Chimaeras

Anabela M.R. Maia, Cheryl A.D. Wilga, and George V. Lauder

CONTENTS

5.1 Introduction

The body form of sharks is notable for the distinctive heterocercal tail with external morphological asymmetry present in most taxa and the ventrolateral winglike pectoral fins extending laterally from the body (Figure 5.1) that give the appearance of powerful yet effortless locomotion. In contrast, expansion of the pectoral fins coupled with a dorsoventrally flattened body in rays and skates resulted in modification of locomotor mode from trunk based to pectoral based, while the chimaera body shape is similar to that of actinopterygian fishes in terms of lateral compression. These features are distinct from the variety of body forms present in actinopterygian fishes (Lauder, 2000) and have long been of interest to researchers wishing to understand the functional design of sharks (Aleev, 1969; Garman, 1913; Grove and Newell, 1936; Harris, 1936; Magnan, 1929; Thomson, 1971).

5.1.1 Approaches to Studying Locomotion in Chondrichthyans

Historically, many attempts have been made to understand the function of the median and paired fins in sharks and rays, and these studies have included work with models (Affleck, 1950; Harris, 1936; Simons, 1970), experiments on fins removed from the body (Aleev, 1969; Alexander, 1965; Daniel, 1922; Harris, 1936), and quantification of body form and basic physical modeling (Thomson, 1976; Thomson and Simanek, 1977). More recently, direct quantification of fin movement using videography has allowed a better understanding of fin conformation and movement (Ferry and Lauder, 1996; Fish and Shannahan, 2000; Flammang, 2010; Wilga and Lauder, 2000), although such studies have to date been limited to relatively few species. Obtaining high-resolution, three-dimensional (3D) data on patterns of shark fin motion is a difficult task, and these studies have

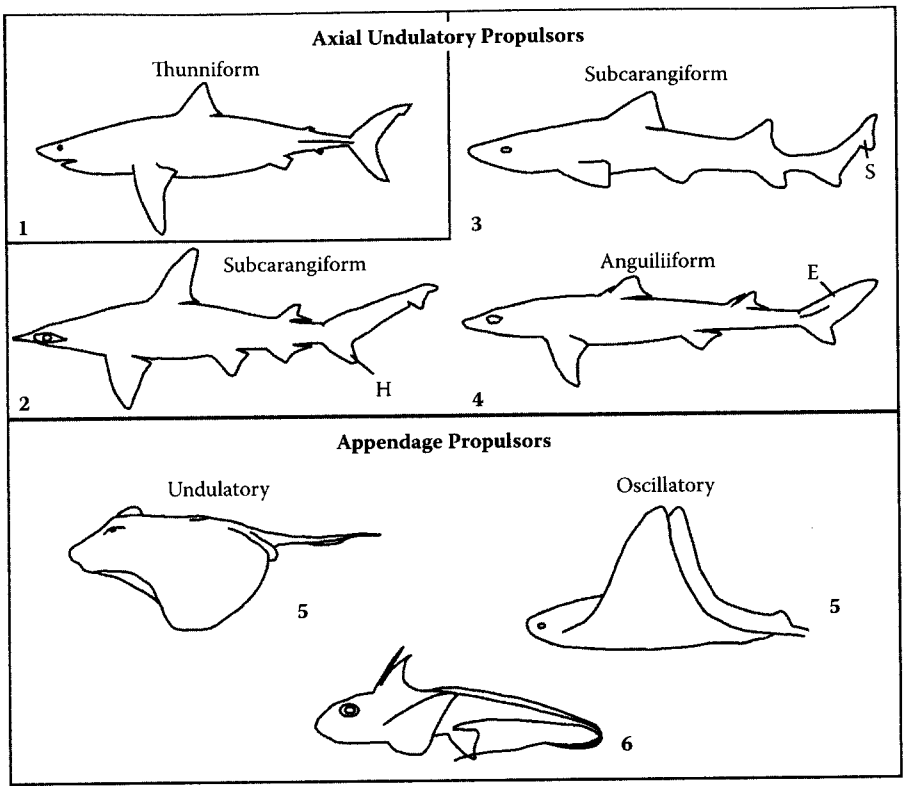

FIGURE 5.1
Propulsion mechanisms in chondrichthyans. Numbers indicate body groups (see text). E, epicaudal lobe; H, hypochordal lobe; S, subterminal lobe. (Based on Webb, 1984; Webb and Blake, 1985.)

been confined to a highly controlled laboratory environment where sharks swim in a recirculating flow tank. Although locomotion of sharks and rays under these conditions does not allow the range of behaviors seen in the wild, the ability to obtain data from precisely controlled horizontal swimming as well as specific maneuvering behaviors has been vital to both testing classical hypotheses of fin function and to the discovery of new aspects of locomotory mechanics. A key general lesson learned from recent experimental kinematic and hydrodynamic analyses of shark locomotion is the value of understanding the 3D pattern of fin movement and the requirement for experimental laboratory studies that permit detailed analyses of fin kinematics and hydrodynamics.

Two new laboratory-based approaches in recent years have been particularly fruitful in clarifying the biomechanics of shark locomotion. Chief among these has been the use of two- and three-camera high-speed video systems to quantify patterns of fin motion in 3D (e.g., Ferry and Lauder, 1996; Standen and Lauder, 2005; Wilga and Lauder, 2000). Two-dimensional (2D) analyses are subject to very large errors when motion occurs in 3D, and the orientation of a planar surface element in 3D can be opposite to the angle appearing in a single 2D view; an example of this phenomenon relevant to the study of shark tails is given in Lauder (2000). The use of two or more simultaneous high-speed video cameras permits determination of the x, y, and z locations of individual points and hence the 3D orientation of fin and body surface elements and distortion to be extracted from the images (Lauder and Madden, 2008). Three-dimensional kinematic analysis has been identified as the new challenge in fish locomotion (Tytell et al., 2008).

The second new approach to studying shark locomotor biomechanics has been the application of flow visualization techniques from the field of fluid mechanics. Briefly, the technique of particle image velocimetry (PIV) (Krothapalli and Lourenco, 1997; Willert and Gharib, 1991) allows direct visualization of water flow around the fins of swimming sharks and quantification of the resulting body and fin wake (e.g., Lauder and Drucker, 2002; Lauder et al., 2003; Wilga and Lauder, 2002). We now have the ability to understand the hydrodynamic significance of different fin and body shapes and to measure forces exerted on the water as a result of fin motion (Lauder and Drucker, 2002). This represents a real advance over more qualitative previous approaches, such as injection of dye to gain an impression of how the fins of fishes function.

Additional techniques that have provided new avenues for research in fish locomotion and are being applied to chondrichthyan locomotion are computational fluid

dynamics (CFD) (Tytell et al., 2010) and material property testing on cartilaginous locomotor structures (Porter and Long, 2010; Porter et al., 2006, 2007; Schaefer and Summers, 2005). Finally, more traditional experimental techniques such as electromyography to quantify the timing of muscle activation, in combination with newer techniques such as sonomicrometry (Donley and Shadwick, 2003; Donley et al., 2005), are revealing new aspects of shark muscle function during locomotion.

5.1.2 Diversity of Locomotory Modes in Chondrichthyans

Sharks, rays, and chimaeras have had a long evolutionary history leading to the locomotor modes observed in extant forms (Carroll, 1988). Chondrichthyans have a remarkable diversity of body forms and locomotor modes for a group containing so few species (Figure 5.1). All sharks swim using continuous lateral undulations of the axial skeleton; however, angel sharks, which are dorsoventrally depressed, may supplement axial propulsion with undulations of their enlarged pectoral fins. Four modes of axial undulatory propulsion have been described, based on decreasing proportion of the body that is undulated during locomotion, which form a continuum from anguilliform to thunniform (Donley and Shadwick, 2003; Webb and Blake, 1985; Webb and Keyes, 1982). In anguilliform swimmers, the entire trunk and tail participate in lateral undulations where more than one wave is present. This mode is characteristic of many elongate sharks such as orectolobiforms, *Chlamydoselachus*, and more benthic carcharhiniform sharks such as scyliorhinids. More pelagic sharks, such as squaliforms, most carcharhiniforms, and some lamniforms, are carangiform swimmers (Breder, 1926; Donley and Shadwick, 2003; Gray, 1968; Lindsey, 1978), whose undulations are mostly confined to the posterior half of the body with less than one wave present. The amplitude of body motion increases markedly over the posterior half of the body (Donley and Shadwick, 2003; Webb and Keyes, 1982). Only the tail and caudal peduncle undulate in thunniform swimmers, which is a distinguishing feature of lamniform sharks, most of which are high-speed cruisers (Donley et al., 2005).

Most batoids (skates and rays) have short, stiff head and trunk regions with slender tails and reduced dorsal fins; therefore, they must swim by moving the pectoral fins. Two modes of appendage propulsion are exhibited by batoids: undulatory and oscillatory (Figure 5.1) (Webb, 1984). Similar to axial swimmers, undulatory appendage propulsors swim by passing undulatory waves down the pectoral fin from anterior to posterior (Daniel, 1922). Most batoids are undulatory appendage propulsors; however, some myliobatiforms, such as eagle and manta rays, swim by flapping their pectoral fins up and down in a mode known as oscillatory appendage propulsion (Rosenberger, 2001). In addition, batoids can augment thrust by punting off the substrate with the pelvic fins (Koester and Spirito, 1999; Macesic and Kajiura, 2010). Holocephalans are appendage propulsors and utilize a combination of flapping and undulation of the pectoral fins for propulsion and maneuvering, much like many teleost fishes (Combes and Daniel, 2001; Foster and Higham, 2010).

5.1.3 Body Form and Fin Shapes

Most species of sharks have a fusiform-shaped body that varies from elongate in species such as bamboo sharks to the more familiar torpedo shape of white sharks; however, angel sharks and wobbegong sharks are dorsoventrally depressed. There is great variability in the morphology of the paired and unpaired fins. Four general body forms have been described for sharks that encompass this variation (Thomson and Simanek, 1977), with two additional body forms that include batoids and holocephalans.

Sharks with body type 1 (Figure 5.1) have a conical head; a large, deep body; large pectoral fins; a narrow caudal peduncle with lateral keels; and a high-aspect-ratio tail (high heterocercal angle) that is externally symmetrical. These are typically fast-swimming pelagic sharks such as *Carcharodon*, *Isurus*, and *Lamna*. As is typical of most high-speed cruisers, these sharks have reduced pelvic, second dorsal, and anal fins, which act to increase streamlining and reduce drag; however, *Cetorhinus* and *Rhincodon*, which are slow-moving filter feeders, also fit into this category. In these sharks, the externally symmetrical tail presumably results in more efficient slow cruising speeds in large-bodied pelagic sharks, aligns the mouth with the center of mass and the center of thrust from the tail, and probably increases feeding efficiency.

Sharks with body type 2 (Figure 5.1) have a more flattened ventral head and body surface, a less deep body, large pectoral fins, and a lower heterocercal tail angle, and they lack keels. These are more generalized, continental swimmers such as *Alopias*, *Carcharias*, *Carcharhinus*, *Galeocerdo*, *Negaprion*, *Prionace*, *Sphyrna*, *Mustelus*, and *Triakis*. *Alopias* is similar to these sharks despite the elongate pectoral and caudal fins. Similarly, hammerheads, with the exception of the cephalofoil, also fit into this category. These sharks probably have the greatest range of swimming speeds. They also retain moderately sized pelvic, second dorsal, and anal fins and therefore remain highly maneuverable over their swimming range.

Sharks with body type 3 (Figure 5.1) have relatively large heads, blunt snouts, more anterior pelvic fins, more posterior first dorsal fins, and a low heterocercal

tail angle with a small to absent hypochordal lobe and a large subterminal lobe. These sharks are slow-swimming epibenthic, benthic, and demersal sharks such as *Scyliorhinus, Ginglymostoma, Chiloscyllium, Galeus, Apristurus, Pseudotriakis,* and Hexanchiformes. Pristiophoriforms and pristiforms may fit best into this category. Although the body morphology of hexanchiform sharks is most similar to these, they have only one dorsal fin that is positioned more posterior on the body than the pelvic fins.

Body type 4 (Figure 5.1) is united by only a few characteristics and encompasses a variety of body shapes. These sharks lack an anal fin and have a large epicaudal lobe. Only squalean or dogfish sharks are represented in this category. Most of these species are deep-sea sharks and have slightly higher pectoral fin insertions (i.e., *Squalus, Isistius, Centroscymnus, Centroscyllium, Dalatius, Echinorhinus, Etmopterus,* and *Somniosus*). *Squalus* also frequent continental waters and have higher aspect tails similar to those in type 2.

A fifth body type (Figure 5.1) can be described based on dorsoventral flattening of the body, enlarged pectoral fins, and a reduction in the caudal half of the body. This type would include batoids, except for pristiforms and guitarfishes. These chondrichthyans are largely benthic but also include the pelagic myliobatiform rays. Rajiforms and myliobatiforms locomote by undulating the pectoral fins, whereas torpediniforms undulate the tail and rhinobatiforms undulate both the pectoral fins and tail.

Holocephalans or chimaeras represent the sixth body type. They resemble teleosts in that they are laterally compressed and undulate the pectoral fins rather than the axial body in steady horizontal swimming. Tail morphology ranges from long and tapering (leptocercal) to distinctly heterocercal.

5.2 Locomotion in Sharks

5.2.1 Function of the Body during Steady Locomotion and Vertical Maneuvering

The anatomy of the various components of shark fin and body musculature and skeleton has previously been reviewed (Bone, 1999; Compagno, 1999; Kemp, 1999; Liem and Summers, 1999) and is not covered again here, where our focus is the biomechanics of fin and body locomotion. It is worth noting, however, that there are very few detailed studies of the musculature and connective tissue within fins and little knowledge of how myotomal musculature is modified at the caudal peduncle (Gemballa et al., 2006; Reif and Weishampel, 1986; Wilga and Lauder, 2001). Such studies will be particularly valuable for understanding how muscular forces are transmitted to paired and median fins.

One of the most important factors in shark locomotion is the orientation of the body, because this is the primary means by which the overall force balance (considered in detail below) is achieved during swimming and maneuvering. When sharks are induced to swim horizontally so that the path of any point on the body is at all times parallel to the x (horizontal) axis with effectively no vertical (y) motion, the body is tilted up at a positive angle of attack to oncoming flow (Figure 5.2). This positive body angle occurs even though sharks are swimming steadily and not maneuvering and are maintaining their vertical position in the water. This positive body angle ranges from 11° to 4° in *Triakis* and *Chiloscyllium*, respectively, at slow swimming speeds of 0.5 *l*/s. The angle of body attack varies with speed, decreasing to near zero at 2 *l*/s swimming speed (Figure 5.2). During vertical maneuvering in the water column, the angle of the body is altered as well (Figure 5.3). When leopard sharks rise so that all body points show increasing values along the y-axis, the body is tilted to a mean angle of 22° into the flow. During sinking in the water, the body is oriented at a negative angle of attack averaging –11° in *Triakis* (Figure 5.3). These changes in body orientation undoubtedly reflect changes in lift forces necessary either to maintain body position given the negative buoyancy of most sharks or to effect vertical maneuvers.

The locomotor kinematics of the body in sharks at a variety of speeds has been studied by Webb and Keyes (1982). Recent studies have presented electromyographic recordings of body musculature to correlate activation patterns of red myotomal fibers with muscle strain patterns and body movement (Donley and Shadwick, 2003; Donley et al., 2005). Red muscle fibers in the body myotomes of *Triakis* are activated to produce the body wave at a consistent relative time all along the length of the body (Donley and Shadwick, 2003). The onset of muscle activation always occurred as the red fibers were lengthening, and these fibers were deactivated consistently during muscle shortening. The authors concluded that the red muscle fibers along the entire length of the body produce positive power and hence contribute to locomotor thrust generation, in contrast to some previous hypotheses suggesting that locomotion in fishes is powered by anterior body muscles alone. Strain in the white axial musculature, which is indicative of force transmission, was measured in mako sharks, *Isurus oxyrinchus* (thunniform swimmers), and showed that there is a decoupling of red muscle activity and local axial bending (Donley et al., 2005). The presence of well-developed hypaxial lateral tendons that differ markedly from those in teleost fishes lends support to this hypothesis (Donley et al., 2005). Recent studies on musculotendinous anatomy revealed

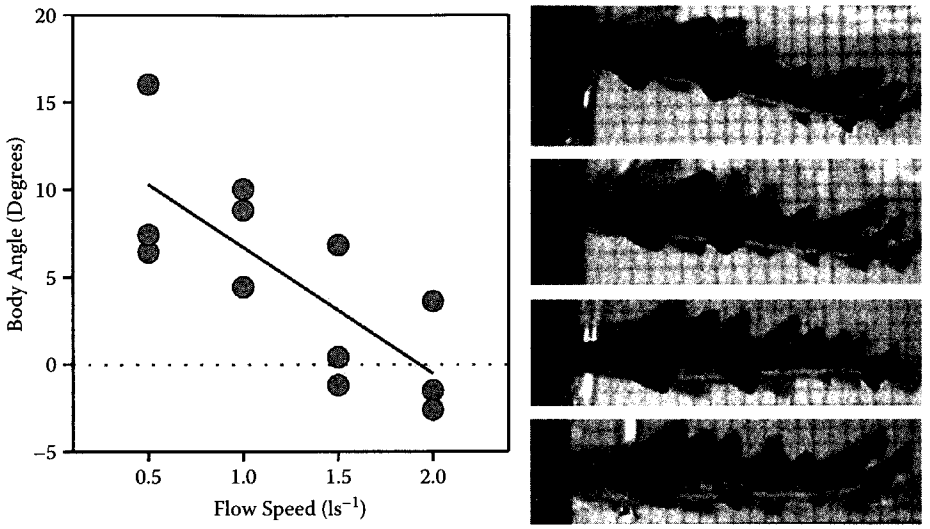

FIGURE 5.2
Plot of body angle vs. flow speed to show the decreasing angle of the body with increasing speed. Each symbol represents the mean of five body angle measurements (equally spaced in time) for five tail beats for four individuals. Images show body position at the corresponding flow speeds in *l*/s, where *l* is total body length (flow direction is left to right). At all speeds, sharks are holding both horizontal and vertical position in the flow and not rising or sinking in the water column. Body angle was calculated using a line drawn along the ventral body surface from the pectoral fin base to the pelvic fin base and the horizontal (parallel to the flow). A linear regression ($y = 15.1 - 7.4x$, adjusted $r^2 = 0.43$, $P < 0.001$) was significant and gives the best fit to the data. (From Wilga, C.D. and Lauder, G.V., *J. Exp. Biol.*, 203, 2261–2278, 2000. With permission.)

significant implications for force transmission in thunniform sharks (Gemballa et al., 2006). This study compared red muscle and tendon changes in subcarangiform to thunniform swimmers. The subcarangiform species have myosepta with one main anterior-pointing cone and two posterior-pointing ones. Within each myoseptum the cones are connected by longitudinal tendons, hypaxial and epaxial lateral tendons, and myorhabdoid tendons, while connection to the skin and vertebral axis is made through epineural and epipleural tendons with a mediolateral orientation. The lateral tendons do not extend more than 0.075 total length (TL) of the shark, and the red muscles insert in the mid-region of these lateral tendons. The thunniform swimmer (mako), however, has a very different condition, thought to have evolved as a result of the demands of this locomotor mode. The

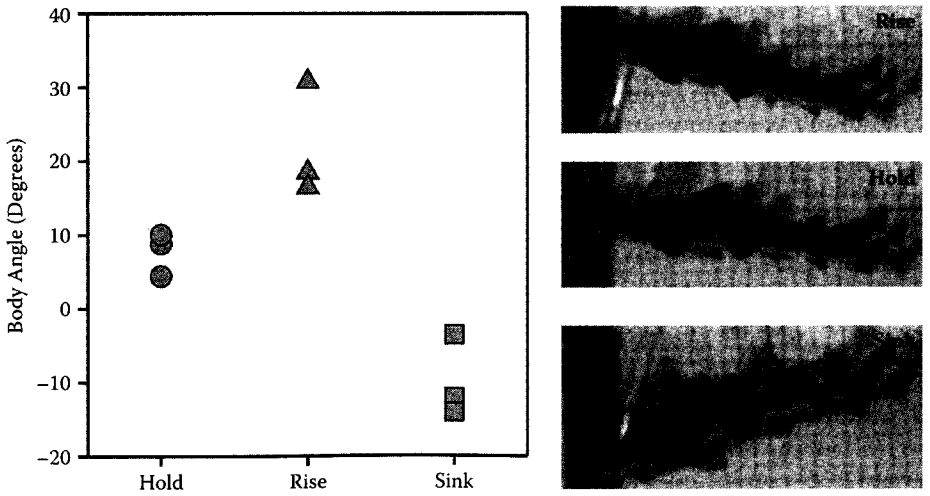

FIGURE 5.3
Plot of body angle vs. behavior during locomotion at 1.0 *l*/s. Circles indicate holding behavior, triangles show rising behavior, and squares reflect sinking behavior. Body angle was calculated as in Figure 5.2. Each point represents the mean of five sequences for each of four individuals. To the right are representative images showing body position during rising, holding, and sinking behaviors. Body angle is significantly different among the three behaviors (ANOVA, $P = 0.0001$). (From Wilga, C.D. and Lauder, G.V., *J. Exp. Biol.*, 203, 2261–2278, 2000. With permission.)

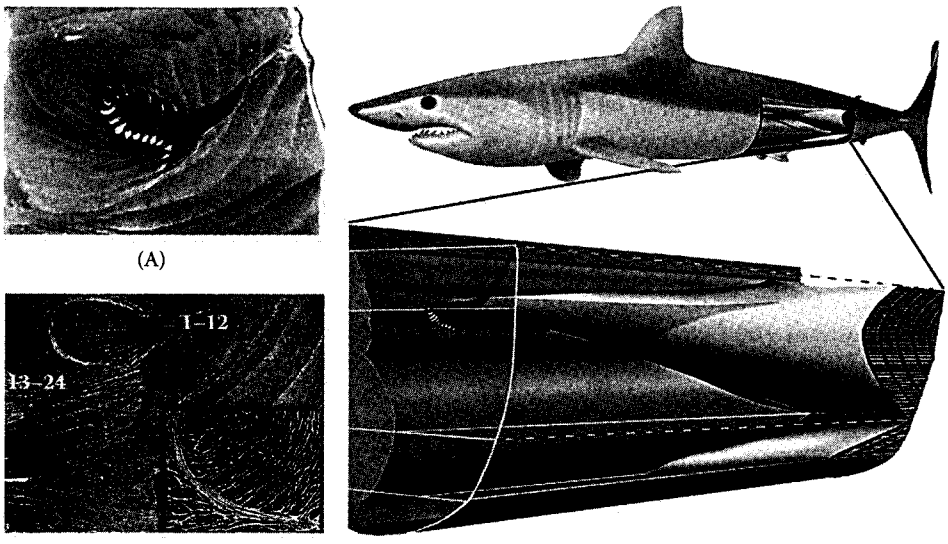

(A) (B) (C)

FIGURE 5.4
Muscle and tendon architecture in a thunniform swimmer, *Isurus oxyrinchus*. (A, B) Transverse sections through main anterior cone and adjacent hypaxial musculature, lateral to the left. (A) Fresh specimen illustrating the deep position of red muscles within the white muscles. (B) Histological section at 0.54 with 24 hypaxial lateral tendons visible (1 to 12 within red muscles, and 13 to 24 within white muscles). Dorso- and ventromedially, the red muscles are separated from the white muscles by a sheath of connective tissue. (C) Three-dimensional reconstruction of a posterior myoseptum. Notice the sections of hypaxial lateral tendons within the red muscle and the correspondence with the sections shown in (A) and (B). (From Gemballa, S. et al., *J. Morphol.*, 267, 477–493, 2006. With permission.)

red muscle is internalized and surrounded by a lubricating connective tissue sheath, and it inserts onto the anterior hypaxial lateral tendon, which increases caudally, spanning as much as 0.19 TL. In addition, the mediolateral fibers are not organized into tendons as in subcarangiform species (Figure 5.4) (Gemballa et al., 2006). Additional specializations for high-speed swimming have been found in salmon sharks, *Lamna ditropis*, which inhabit cold waters and have internalized red muscle that function at elevated temperatures (20°C and 30°C); thus, this species is closer to mammals in muscle activity (Bernal et al., 2005). Magnetic resonance imaging (MRI) was used to determine the position and volume of internalized red muscle in salmon sharks and confirmed the position of the hypaxial lateral tendons that transmit force to the caudal peduncle (Perry et al., 2007).

During propulsion and maneuvering in sharks, skates, and rays, both median fins (caudal, dorsal, and anal) as well as paired fins (pectoral and pelvic) play an important role. In this chapter, however, we focus on the caudal and pectoral fins, as virtually nothing quantitative is known about the function of dorsal, anal, and pelvic fins. Harris (1936) conducted specific experiments designed to understand the function of multiple fins using model sharks placed in an unnatural body position in a wind tunnel. The first dorsal fin in white sharks, *Carcharodon carcharias*, has been hypothesized to function as a dynamic stabilizer during steady swimming based on dermal fiber arrangement, which may allow internal hydrostatic pressure to increase (Lingham-Soliar, 2005). The role of the dorsal, anal, and pelvic fins during locomotion in elasmobranchs is a key area for future research on locomotor mechanics.

5.2.2 Function of the Caudal Fin during Steady Locomotion and Vertical Maneuvering

Motion of the tail is an important aspect of shark propulsion, and the heterocercal tail of sharks moves in a complex 3D manner during locomotion. Ferry and Lauder (1996) used two synchronized high-speed video cameras to quantify the motion of triangular segments of the leopard shark tail during steady horizontal locomotion. Sample video frames from that study, shown in Figure 5.5, illustrate tail position at six times during half of a tail stroke. One video camera viewed the tail laterally, giving the x and y coordinates of identified locations on the tail, while a second camera aimed at a mirror downstream of the tail provided a posterior view, giving z and y coordinates for those same locations. Tail marker locations were connected into triangular surface elements (Figure 5.6A,B), and their orientation was tracked through time. This approach is discussed in more detail by Lauder (2000). Analysis of surface element movement through time showed that for the majority of the tail beat cycle the caudal fin surface was inclined at an angle greater than 90° to the horizontal (Figure 5.6), suggesting that the downwash

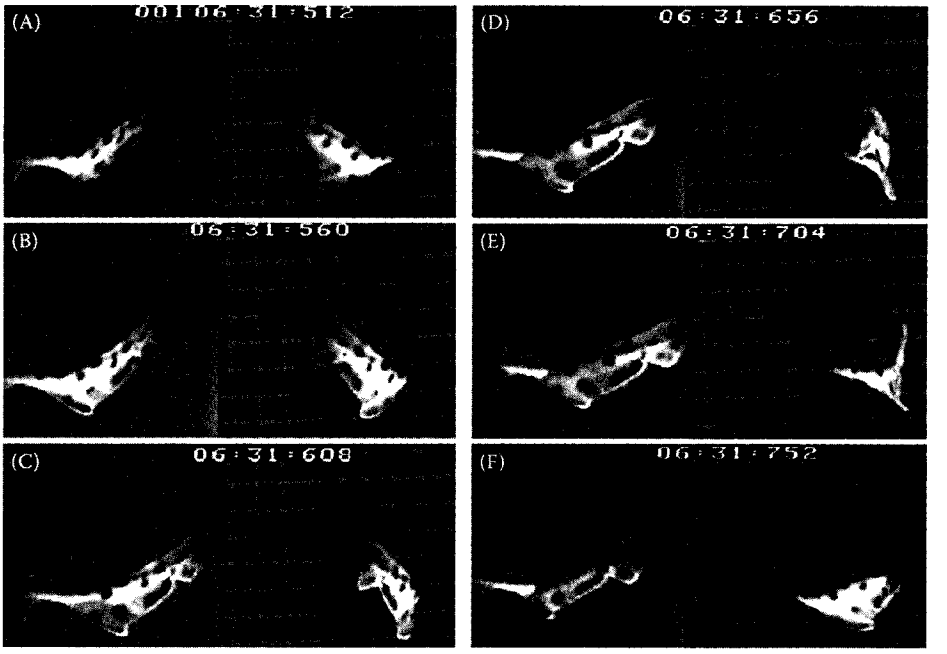

FIGURE 5.5
Composite video sequence of the tail beating from the leftmost extreme (A), crossing the midline of the beat (B, C, and D), and beating to the rightmost extreme or maximum lateral excursion (reached in E and F). In (F), the tail has started its beat back to the left. Times for each image are shown at the top, with the last three digits indicating elapsed time in milliseconds. Each panel contains images from two separate high-speed video cameras, composited into a split-screen view. (From Ferry, L.A. and Lauder, G.V., *J. Exp. Biol.*, 199, 2253–2268, 1996. With permission.)

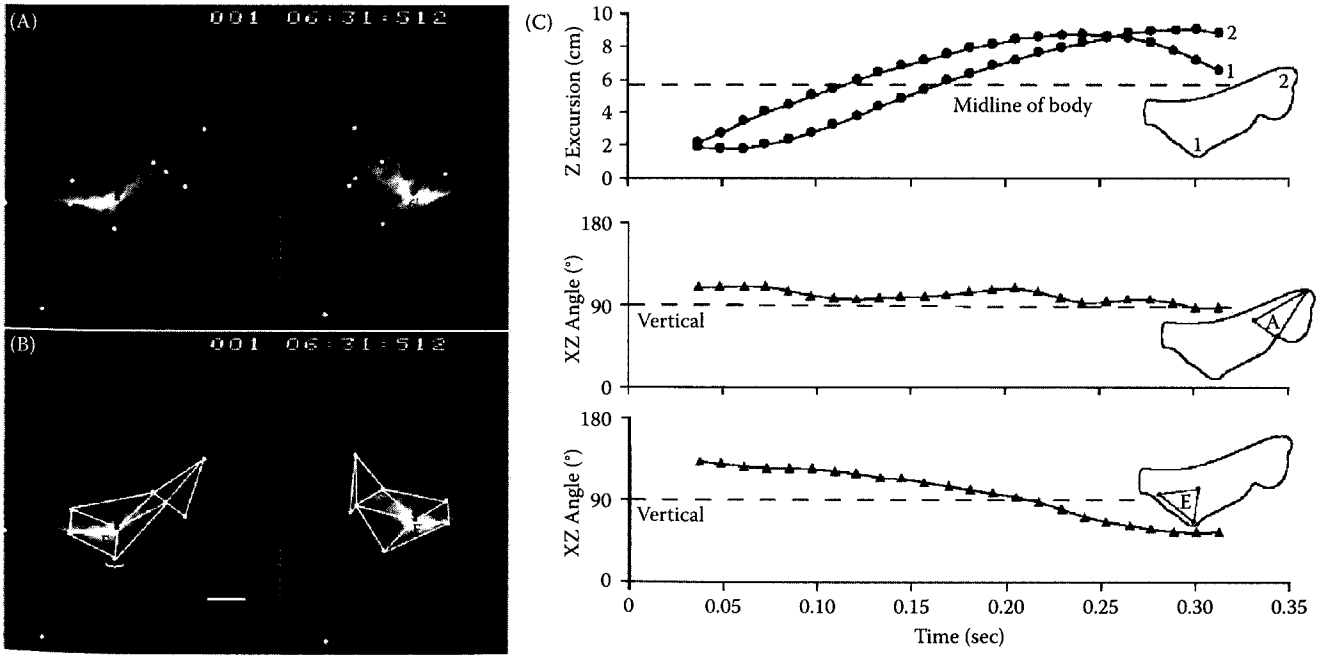

FIGURE 5.6
Images of the tail of a representative leopard shark, *Triakis semifasicata*, swimming in the flow tank. Landmarks (1–8) are shown in (A) with both lateral and posterior views and in (B) with the points joined to form the triangles (A–H) for analysis. Points marked "ref" were digitized as reference points. Both views were identically scaled using the grid in the lateral view (1 box = 2 cm); the smaller grid visible in the posterior view is the upstream baffle reflected in the mirror toward which the shark is swimming. (C) Heterocercal tail kinematics in a representative leopard shark swimming steadily at 1.2 *l*/s; *z*-dimension excursions (upper panel) of two points on the tail and the three-dimensional angles of two tail triangles with the *xz* plane. Note that for most of the tail beat, the orientation of these two triangular elements is greater than 90°, indicating that the tail is moving in accordance with the classical model of heterocercal tail function. (From Ferry, L.A. and Lauder, G.V., *J. Exp. Biol.*, 199, 2253–2268, 1996; Lauder, G.V., *Am. Zool.*, 40, 101–122, 2000. With permission.)

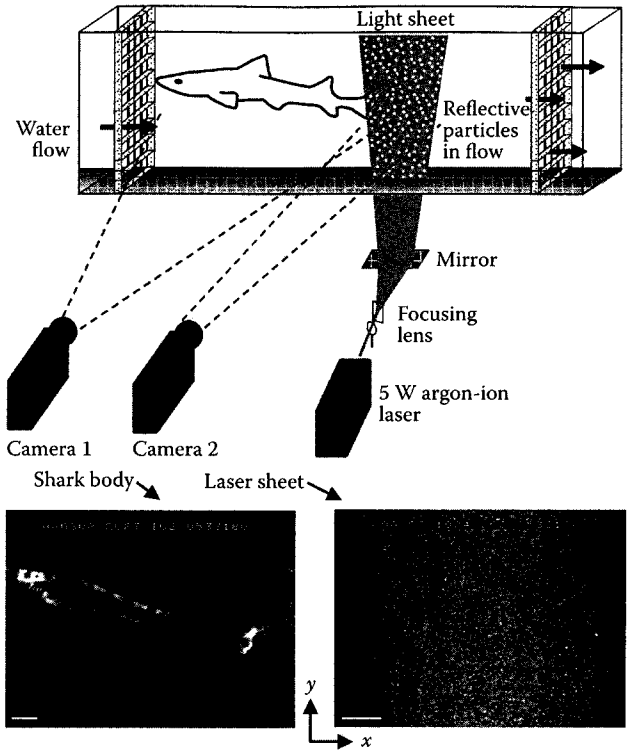

FIGURE 5.7
Schematic diagram of the working section of the flow tank illustrating the defocusing digital particle image velocimetry (DDPIV) system. Sharks swam in the working section of the flow tank with the laser sheet oriented in a vertical (parasagittal, *xy*) plane. Lenses and mirrors were used to focus the laser beam into a thin light sheet directed vertically into the flow tank. The shark is shown with the tail cutting through the laser sheet. Two high-speed video cameras recorded synchronous images of the body (camera 1) and particles in the wake (camera 2) of the freely swimming sharks.

of water from the moving tail would be directed posteroventrally. These data provided kinematic corroboration of the classical model of shark heterocercal tail function, which hypothesized that the shark caudal fin would generate both thrust and lift by moving water posteriorly and ventrally (Alexander, 1965; Grove and Newell, 1936; Lauder, 2000).

Although kinematic data provide strong evidence in support of the classical view of heterocercal tail function in sharks, they do not address what is in fact the primary direct prediction of that model: the direction of water movement. To determine if the heterocercal tail of sharks functions hydrodynamically as expected under the classical view, a new technique is needed that permits direct measurement of water flow. Particle image velocimetry (PIV) is such a technique, and a schematic diagram of this approach as applied to shark locomotion is illustrated in Figure 5.7. Sharks swim in a recirculating flow tank, which has been seeded with small (12-μm mean diameter) reflective hollow glass beads. A 5- to 10-W laser is focused into a light sheet 1 to 2 mm thick and 10 to 15 cm wide, and this beam is aimed into the flow tank using focusing lenses and mirrors. Sharks are induced to swim with the tail at the upstream edge of the light sheet so the wake of the shark passes through the light sheet as this wake is carried downstream. Generally, a second synchronized high-speed video camera takes images of the shark body so orientation and movements in the water column can be quantified.

Analysis of wake flow video images proceeds using standard PIV processing techniques, and further details of PIV as applied to problems in fish locomotion are provided in a number of recent papers (Drucker and Lauder, 1999, 2005; Lauder, 2000; Lauder and Drucker, 2002; Lauder et al., 2002, 2003; Nauen and Lauder, 2002; Standen, 2010; Standen and Lauder, 2005, 2007; Wilga and Lauder, 1999, 2000, 2001, 2002). Briefly, cross-correlation of patterns of pixel intensity between homologous regions of images separated in time is used to generate a matrix of velocity vectors, which reflect the pattern of fluid flow through the light sheet. Commercial and freeware versions of PIV analysis software are available and used widely (Raffel et al., 2007; Stamhuis, 2006). Sample PIV data are presented in Figure 5.8. From these matrices of velocity vectors the orientation of fluid accelerated by the tail can be quantified and any rotational movement measured as fluid vorticity. Recent research on fish caudal fin function has shown that the caudal

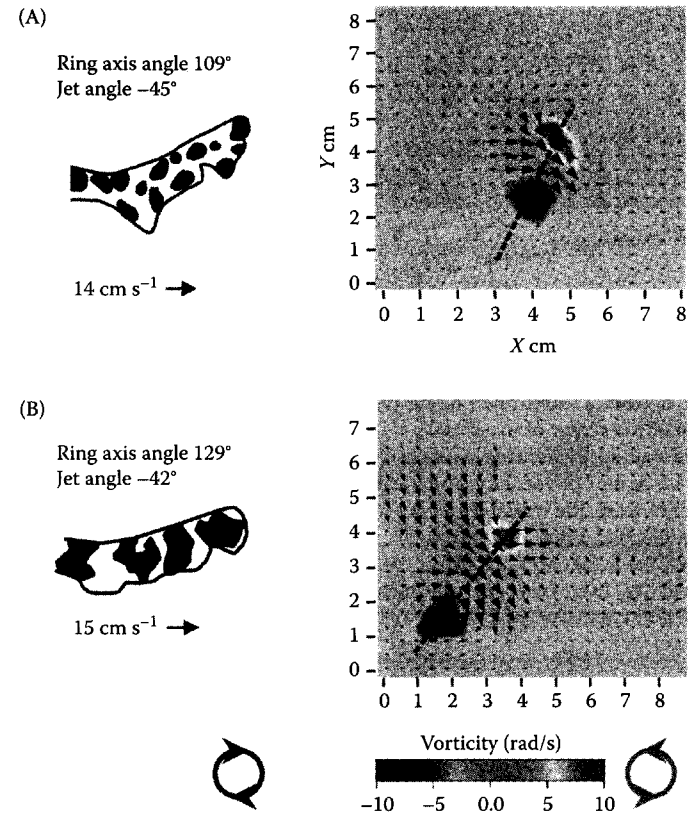

FIGURE 5.8
Defocusing digital particle image velocimetry (DDPIV) analysis of the wake of the tail of representative (A) *Triakis semifasciata* and (B) *Chiloscyllium punctatum* sharks during steady horizontal locomotion at 1.0 *l*/s. On the left is a tracing depicting the position of the tail relative to the shed vortex ring visible in this vertical section of the wake. The plot to the right shows fluid vorticity with the matrix of black velocity vectors representing the results of DPIV calculations based on particle displacements superimposed on top. A strong jet, indicated by the larger velocity vectors, passes between two counterrotating vortices representing a slice through the vortex ring shed from the tail at the end of each beat. The black dashed line represents the ring axis angle. *Note:* Light gray color indicates no fluid rotation, dark gray color reflects clockwise fluid rotation, and medium gray color indicates counterclockwise fluid rotation. To assist in visualizing jet flow, a mean horizontal flow of $u = 19$ and $u = 24$ cm/s was subtracted from each vector for *T. semifasciata* and *C. punctatum*, respectively. (From Wilga, C.D. and Lauder, G. V., *J. Exp. Biol.*, 205, 2365–2374, 2002. With permission.)

fin of fishes sheds momentum in the form of vortex loops as the wake rolls up into discrete torus-shaped rings with a central high-velocity jet flow (Drucker and Lauder, 1999; Lauder and Drucker, 2002). By quantifying the morphology of these wake vortex rings, we can determine the direction of force application to the water by the heterocercal tail by measuring the direction of the central vortex ring momentum jet. In addition, the absolute force exerted on the water by the tail can be calculated by measuring the strength and shape of the vortex rings (Dickinson, 1996; Drucker and Lauder, 1999; Lauder and Drucker, 2002).

Using the two-camera arrangement illustrated in Figure 5.7, Wilga and Lauder (2002) studied the hydrodynamics of the tail of leopard sharks during both steady horizontal locomotion and vertical maneuvering. They measured the orientation of the body relative to the horizontal, the path of motion of the body through the water, and the orientation and hydrodynamic characteristics of the vortex rings shed by the tail (Figure 5.9). Representative data from that study are shown in Figure 5.8, which illustrates the pattern of water velocity and vortex ring orientation resulting from one tail beat in two species of sharks. Tail vortex rings are inclined significantly to the vertical and are tilted posterodorsally. The central high-velocity water jet through the center of each vortex ring is oriented posteroventrally at an angle between 40° and 45° below the horizontal. These data provide unequivocal support for the classical model of heterocercal tail function in sharks by demonstrating that the tail accelerates water posteroventrally and that there must necessarily be a corresponding reaction force with dorsal (lift) and anterior (thrust) components.

Analysis of the changing orientation of tail vortex rings as sharks maneuver vertically in the water demonstrates that the relationship between vortex ring

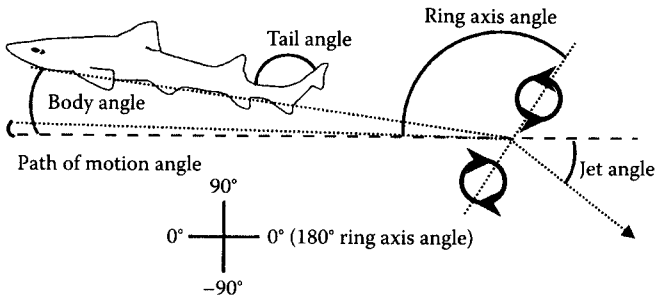

FIGURE 5.9
Schematic summary illustrating body and wake variables measured relative to the horizontal: body angle, from a line drawn along the ventral body surface; path of motion of the center of mass; tail angle between the caudal peduncle and dorsal tail lobe; ring axis angle, from a line extending between the two centers of vorticity; and mean vortex jet angle. Angle measurements from the variables of interest (dotted lines) to the horizontal (dashed line) are indicated by the curved solid lines. Angles above the horizontal are considered positive and below the horizontal negative. Ring axis angle was measured from 0° to 180° (From Wilga, C.D. and Lauder, G. V., *J. Exp. Biol.*, 205, 2365–2374, 2002. With permission.)

angle and body angle remains constant as body angle changes during maneuvering (Figure 5.10). These data show that leopard sharks do not alter the direction of force application to the water by the tail during vertical maneuvering, in contrast to previous data from sturgeon that demonstrated the ability to actively alter tail vortex wake orientation as they maneuver (Liao and Lauder, 2000).

A newly described intrinsic radialis tail muscle may function to stiffen the fin to change tail conformation (Flammang, 2010). The radialis muscle extends ventral to the axial myomeres and is composed of red fibers angled dorsoposteriorly. A similar arrangement exists in all sharks examined, with slight changes in angel sharks and rays and absence in skates and chimaeras. Muscle activity in spiny dogfish at slow speed follows an anterior to posterior pattern prior to activation of red axial muscle in the caudal myomeres (Figure 5.11). In contrast, at higher speed, only the anterior portion of the radialis muscle shows activity (Flammang, 2010).

5.2.3 Function of the Pectoral Fins during Locomotion

5.2.3.1 Anatomy of the Pectoral Fins

There are two distinct types of pectoral fins in sharks based on skeletal morphology. In aplesodic fins, the cartilaginous radials are blunt and extend up to 50% into the fin with the distal web supported only by ceratotrichia. In contrast, plesodic fins have radials that extend more than 50% into the fin to stiffen it and supplement the support of the ceratotrichia (Compagno, 1988) (Figure 5.12). The last row of radials tapers to a point distally in plesodic fins. Plesodic fins appear in Lamniformes, hemigaleids, carcharhinids, sphyrnids, and batoids except for pristids; other groups have aplesodic fins (Shirai, 1996). The restricted distribution of plesodic pectoral fins in extant sharks, the different morphology in each group, and their occurrence in more derived members (by other characters) of each group strongly suggest that plesodic pectorals are derived and have evolved independently from aplesodic pectorals (Bendix-Almgreen, 1975; Compagno, 1973, 1988; Zangerl, 1973). The decreased skeletal support of aplesodic pectoral fins over plesodic fins

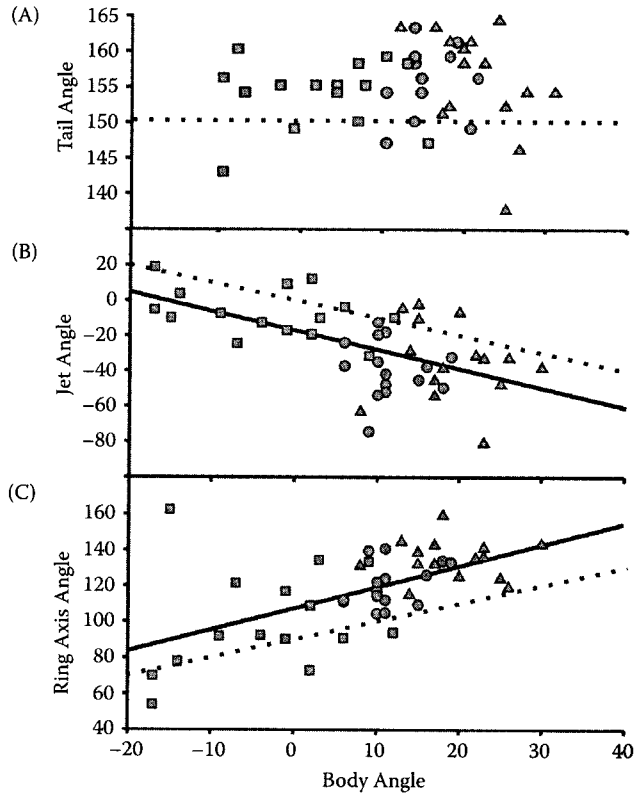

FIGURE 5.10
Plot of body angles. (A) Tail angle, (B) jet angle, and (C) ring axis angle in leopard sharks, *Triakis semifasciata*, while swimming at 1.0 *l*/s. Solid lines indicate a significant linear regression, and the dotted line represents the predicted relationship. The lack of significance of the tail vs. body angle regression ($P = 0.731$, $r^2 = 0.003$) indicates that the sharks are not altering tail angle as body angle changes but instead are maintaining a constant angular relationship regardless of locomotor behavior. Jet angle decreases with increasing body angle ($P < 0.001$, $r^2 = 0.312$, $y = -17 - 1.087x$) at the same rate as the predicted parallel relationship, indicating that the vortex jet is generated at a constant angle to the body regardless of body position. Ring axis angle increases with body angle at the same rate as the predicted perpendicular relationship ($P < 0.001$, $r^2 = 0.401$, $y = 107 + 1.280x$). Circles, triangles, and squares represent holds, rises, and sinks, respectively. (From Wilga, C.D. and Lauder, G. V., *J. Exp. Biol.*, 205, 2365–2374, 2002. With permission.)

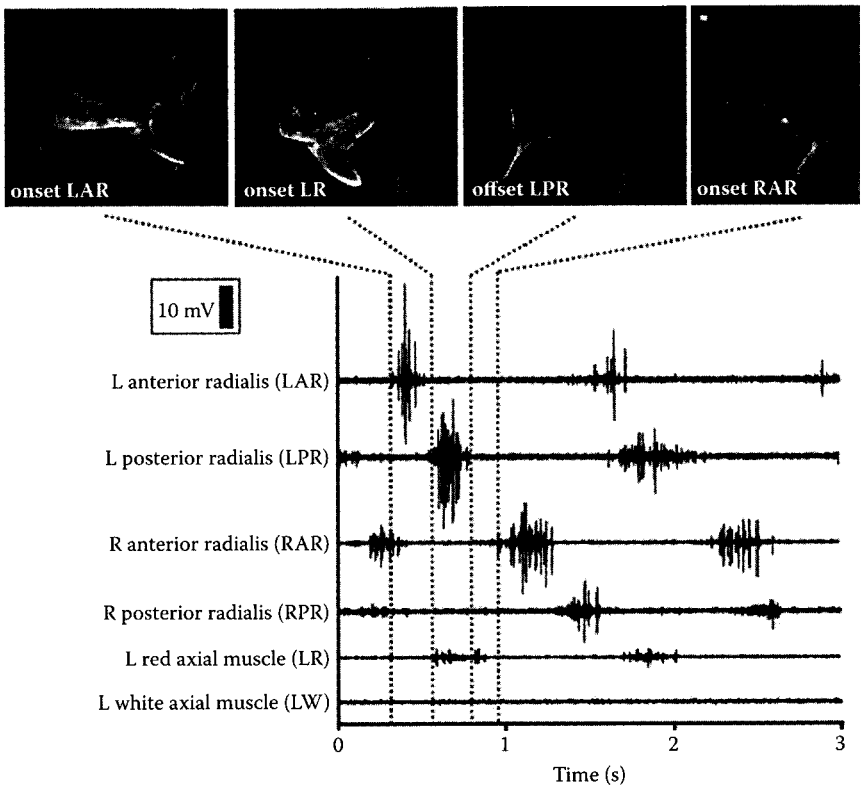

FIGURE 5.11
Tail kinematics and electromyographic recordings of tail muscles of a spiny dogfish swimming steadily at 0.5 *l*/s. Note the anterior to posterior activation of the radialis muscle. (From Flammang, B.E., *J. Morphol.*, 271, 340–352, 2010. With permission.)

allows greater freedom of motion in the distal web of the fin and may function to increase maneuverability. *Chiloscyllium* (Orectolobiformes) frequently "walk" on the substrate using both the pectoral and pelvic fins (Pridmore, 1995) in a manner similar to that of salamanders. They can bend the pectoral fins such that an acute angle is formed ventrally when rising on the substrate, and angles up to 165° are formed dorsally when station-holding on the substrate. *Chiloscyllium* are even able to walk backward using both sets of paired fins (AMRM and CDW, pers. obs.). In contrast, the increased skeletal support of plesodic fins stiffens and streamlines the distal web, which reduces drag. Furthermore, the extent of muscle insertion into the pectoral fin appears to correlate with the extent of radial support into the fin and thus pectoral fin type. In sharks with aplesodic fins, the pectoral fin muscles insert as far as the third (and last) row of radial pterygiophores, well into the fin. In contrast, those sharks with plesodic fins have muscles that insert only as far as the second row (of three) of radials.

Streamlined rigid bodies are characteristic of fishes that are specialized for cruising and sprinting, whereas flexible bodies are characteristic of fishes that are specialized for accelerating or maneuvering (Webb, 1985, 1988). Applying this analogy to shark pectoral fins, it may be that plesodic fins are specialized for cruising (fast-swimming pelagic sharks) and aplesodic fins are specialized for accelerating or maneuvering (slow-cruising pelagic and benthic sharks).

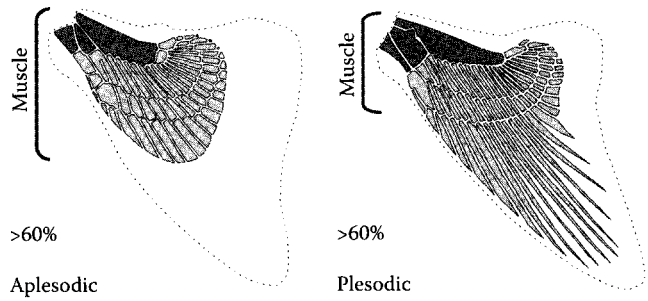

FIGURE 5.12
(Left) Skeletal structure of the pectoral fins in aplesodic sharks, such as leopard, bamboo, and dogfish (Wilga and Lauder, 2001); (right) plesodic sharks, such as lemon, blacktip, and hammerhead (redrawn from Compagno, 1988). The left pectoral fin for each species is shown in dorsal view. Dark gray elements are propterygium, mesopterygium, and metapterygium from anterior to posterior; light gray elements are radials. The dotted line delimits the extent of ceratotrichia into the fin web. Muscle insertion extends to the end of the third row of radials in aplesodic sharks and to the end of the second row or middle of the third row of radials in plesodic sharks.

5.2.3.2 Role of the Pectoral Fins during Steady Swimming

The function of the pectoral fins during steady horizontal swimming and vertical maneuvering (rising and sinking) has been tested experimentally in *Triakis semifasciata*, *Chiloscyllium plagiosum*, and *Squalus acanthias* (Wilga and Lauder, 2000, 2001, 2004). Using 3D kinematics and fin marking (Figure 5.13), these studies have shown that the pectoral fins of these sharks are held in such a way that negligible lift is produced during steady horizontal locomotion. The pectoral fins are cambered with an obtuse dorsal angle between the anterior and posterior regions of the fin (mean, 190° to 191°) (Figure 5.14). Thus, the planar surface of the pectoral fin is held concave downward relative to the flow during steady swimming (Figure 5.15), as well as concave mediolaterally.

The posture of the pectoral fins relative to the flow during steady horizontal swimming in these sharks contrasts markedly to those of the wings in a cruising passenger aircraft. The anterior and posterior planes of the pectoral fins in these sharks during steady horizontal swimming are at negative and positive angles, respectively, to the direction of flow (Figure 5.15). When both planes are considered together, the chord angle is –4° to –5° to the flow. Conversely, the wings of most cruising passenger aircraft have a positive attack angle to the direction of oncoming air, which generates positive lift.

The planar surface of the pectoral fins of these sharks is held at a negative dihedral angle (fin angle relative to the horizontal) from –6° (*Chiloscyllium plagiosum*) to –23° (*Triakis semifasciata*) during steady horizontal swimming (Figure 5.16). The pectoral fins are destabilizing in this position (Simons, 1994; Smith, 1992; Wilga and Lauder, 2000) and promote rolling motions of the body, such as

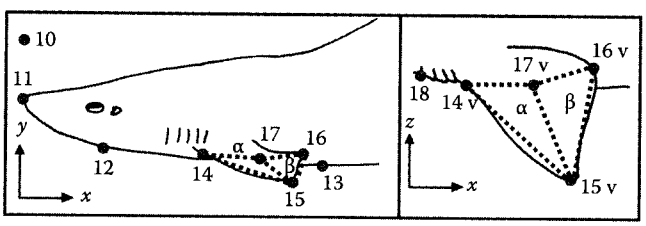

FIGURE 5.13
Schematic diagram of a shark illustrating the digitized points on the body and pectoral fin. Lateral view of the head and pectoral fin (left) and ventral view of pectoral fin region (right). Note that the reference axes differ for lateral (*x*,*y*) and ventral (*x*,*z*) views. Data from both views were recorded simultaneously. Points 14 to 16 are the same points in lateral and ventral views, and points 17 and 17v represent the same location on the dorsal and ventral fin surfaces. These three-dimensional coordinate data were used to calculate a three-dimensional planar angle between the anterior and posterior fin planes (α and β), as shown in B. (From Wilga, C.D. and Lauder, G.V., *J. Exp. Biol.*, 203, 2261–2278, 2000. With permission.)

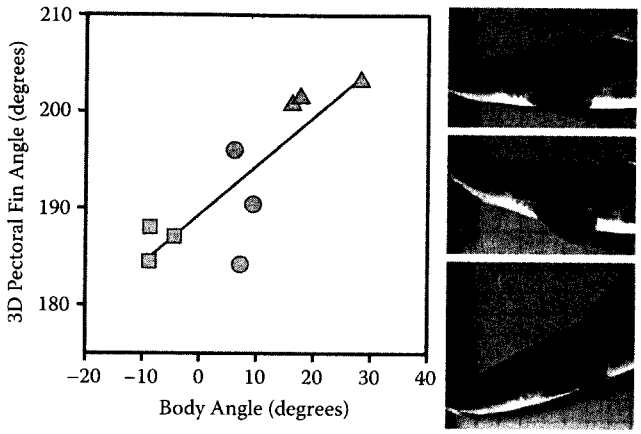

FIGURE 5.14
Graph of three-dimensional pectoral fin angle vs. body angle for rising, holding, and sinking behaviors at 1.0 *l*/s in leopard sharks. Symbols are as in Figure 5.3. Body angle was calculated using the line connecting points 12 and 13 (see Figure 5.11) and the horizontal (parallel to the flow). Each point represents the mean of five sequences for each of four individuals. Images to the right show sample head and pectoral fin positions during each behavior. Pectoral fin angles equal to 180° indicate that the two fin triangles (see Figure 5.11) are coplanar; angles less than 180° indicate that the fin surface is concave dorsally; and angles greater than 180° indicate that the fin surface is concave ventrally. The three-dimensional internal pectoral fin angle is significantly different among the three behaviors (ANOVA, P = 0.0001). The least-squares regression line is significant (slope, 0.41; adjusted r^2 = 0.39; P < 0.001). (From Wilga, C.D. and Lauder, G.V., *J. Exp. Biol.*, 203, 2261–2278, 2000. With permission.)

those made while maneuvering in the water column. For example, in a roll, the fin with the greatest angle to the horizontal meets the flow at a greater angle of attack, resulting in a greater force (F_x) directed into the roll, while the angle of attack of the more horizontally oriented fin is reduced by the same amount. This is in direct contrast to previous studies suggesting that the pectoral fins of sharks are oriented to prevent rolling, as in the keel of a ship (Harris, 1936, 1953). Wings that are tilted at a positive angle with respect to the horizontal have a positive dihedral angle, as in passenger aircraft, and are self-stabilizing in that they resist rolling motions of the fuselage (Figure 5.16) (Simons, 1994; Smith, 1992). When a passenger aircraft rolls, the more horizontally oriented wing generates a greater lift force than the inclined wing (Simons, 1994; Smith, 1992). In this way, a corrective restoring moment arises from the more horizontal wing, which opposes the roll, and the aircraft is returned to the normal cruising position. Interestingly, the negative dihedral wings of fighter aircraft, which are manufactured for maneuverability, function similarly to shark pectoral fins.

The flow of water in the wake of the pectoral fins during locomotion in these three species was quantified using PIV to estimate fluid vorticity and the forces exerted by the fin on the fluid (see Drucker and Lauder,

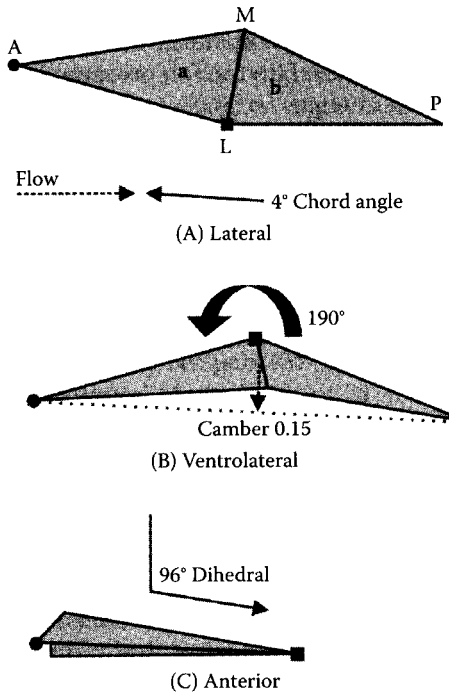

FIGURE 5.15
Orientation of the two pectoral fin planes (*a* and *b*) in three-dimensional space during pelagic holding in bamboo sharks, *Chiloscyllium plagiosum* (leopard and dogfish sharks show similar conformations). Panels show (A) lateral, (B) ventrolateral, and (C) posterior views of the fin planes. Points defining the fin triangles correspond to the following digitized locations in Figure 5.11: A, anterior, point 14, black circle; L, point 15, black square; P, posterior, point 16; M, medial, point 17. Chord angle to the flow is given in the lateral view, camber and internal fin angles between planes *a* and *b* are given in the ventrolateral view, and the dihedral angle is shown in the posterior view. (Note that in the posterior view the angles are given as acute to the *xy* plane.) (From Wilga, C.D. and Lauder, G.V., *J. Morphol.*, 249, 195–209, 2001. With permission.)

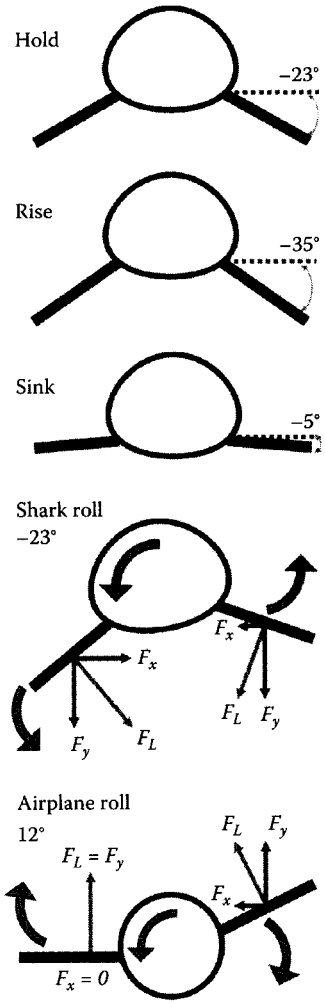

FIGURE 5.16
Schematic diagram of the dihedral orientation of the pectoral fins in a shark during holding, rising, and sinking behaviors. Forces during a roll are illustrated below for the pectoral fins of a shark and the wings of an airplane. The body and fin are represented as a cross-section at the level of plane α of the pectoral fin (see Figure 5.11). Thin, gray, double-headed arrows represent the dihedral angle between the plane α (dotted line) and pectoral fin. Thick arrows show the direction of movement of the body and fins or wing during a roll. Note that positive dihedrals (such as those used in aircraft design) are self-stabilizing, while fins oriented at a negative dihedral angle, as in sharks, are destabilizing in roll and tend to amplify roll forces. F_x, horizontal force; F_y, vertical force; F_L, resultant force. (From Wilga, C.D. and Lauder, G.V., *J. Exp. Biol.*, 203, 2261–2278, 2000. With permission.)

1999; Wilga and Lauder, 2000). These results further corroborate the conclusion from the 3D kinematic data that the pectoral fins generate negligible lift during steady horizontal swimming. There was virtually no vorticity or downwash detected in the wake of the pectoral fins during steady horizontal swimming, which shows that little or no lift is being produced by the fins (Figure 5.17). According to Kelvin's law, vortices shed from the pectoral fin must be equivalent in magnitude but opposite in direction to the theoretical bound circulation around the fin (Dickinson, 1996; Kundu, 1990); therefore, the circulation of the shed vortex can be used to estimate the force on the fin. Mean downstream vertical fluid impulse calculated in the wake of the pectoral fins during steady horizontal swimming was not significantly different from zero. This indicates that the sharks are holding their pectoral fins in such a way that the flow speed and pressure are equivalent on the dorsal and ventral surfaces of the fin. Furthermore, if the pectoral fins were generating lift to counteract moments generated by the heterocercal tail, there would necessarily be a downwash behind the wing to satisfy Kelvin's law. The lack of an observable and quantifiable downwash indicates clearly that, during holding behavior, pectoral fins generate negligible lift.

These results showing that the pectoral fins of these sharks do not generate lift during steady forward swimming stand in stark contrast to previous findings on sharks with bound or amputated fins (Aleev, 1969;

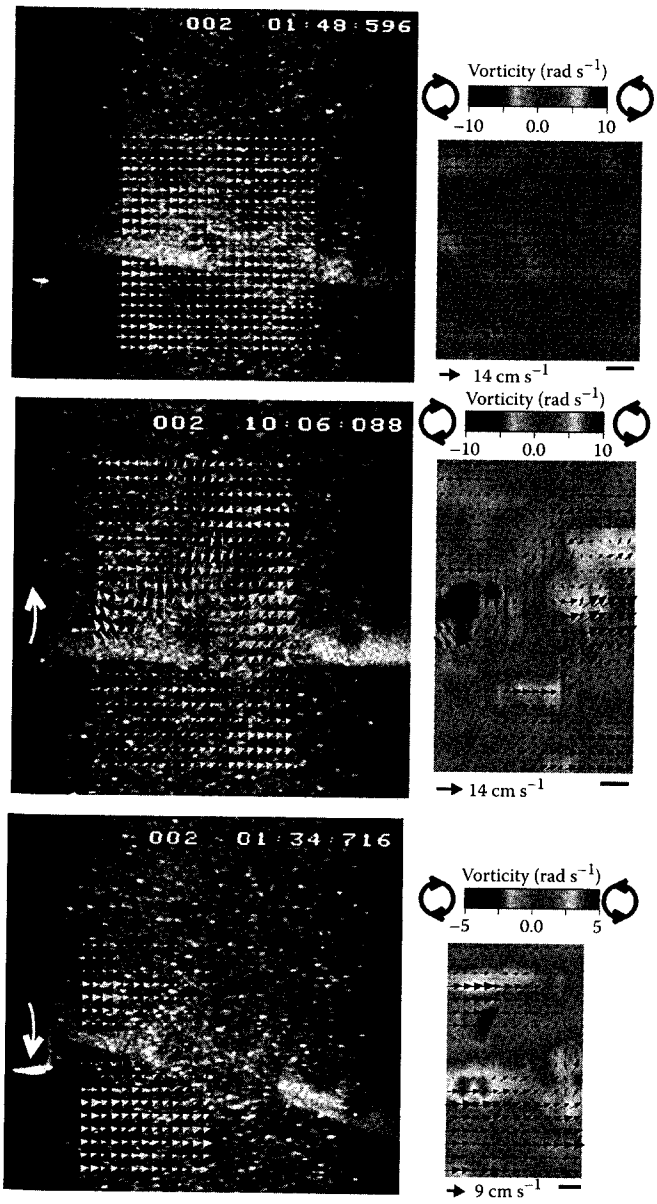

FIGURE 5.17
DPIV data from leopard shark pectoral fins during (top) holding vertical position, (middle) sinking, and (bottom) rising behaviors at 1.0 *l*/s (patterns for bamboo and dogfish sharks are similar). The video image (on the left) is a single image of a shark with the left pectoral fin located just anterior to the laser light sheet. Note that the ventral body margin is faintly visible through the light sheet. The plot on the right shows fluid vorticity with velocity vectors with conventions as in Figure 5.8. Note that the fin in the holding position is held in a horizontal position, and that the vorticity plot shows effectively no fluid rotation. Hence, the pectoral fins in this position do not generate lift forces. During sinking, note that there is a clockwise vortex (dark gray region of rotating fluid to the right) that resulted from the upward fin flip (curved white arrow) to initiate the sinking event. During rising, note that the fin has flipped ventrally (curved white arrow) to initiate the rising event and that a counterclockwise vortex (medium gray region of rotating fluid to the right) has been shed from the fin. To assist in visualizing the flow pattern, a mean horizontal flow of $U = 33$ cm/s was subtracted from each vector. (Adapted from Wilga, C.D. and Lauder, G.V., *J. Morphol.*, 249, 195–209, 2001.)

Daniel, 1922; Harris, 1936). Although the results of such radical experiments are difficult to evaluate, it is likely that the lack of pectoral fin motion prevented the sharks from initiating changes in pitch and therefore limited their ability to achieve a horizontal position and adjust to perturbances in oncoming flow. Lift forces measured on the pectoral fins and body of a plaster model of *Mustelus canis* in a wind tunnel also suggested that the pectoral fins generated upward lift while the body generated no lift (Harris, 1936). However, the pectoral fins were modeled as rigid flat plates (2D) and tilted upward 8° to the flow, while the longitudinal axis of the body was oriented at 0° to the flow. Although it is possible that *M. canis* locomotes with the body and pectoral fins in this position, the results of current studies on live, freely swimming, and closely related *Triakis semifasciata*, which has a very similar body shape, show a radically different orientation of the body and pectoral fins.

Three-dimensional kinematic analyses of swimming organisms are crucial to deriving accurate hypotheses about the function of the pectoral fins and body (Wilga and Lauder, 2000). The 2D angle of the anterior margin of the pectoral fin as a representation of the planar surface of the pectoral fin in sharks is extremely misleading. Although the pectoral fin appears to be oriented at a positive angle to the flow in lateral view, 3D kinematics reveals that the fin is actually concave downward with a negative dihedral. When viewed laterally, this negative-dihedral, concave-downward orientation of the pectoral fin creates a perspective that suggests a positive angle of attack when the angle is, in fact, negative.

5.2.3.3 Role of the Pectoral Fins during Vertical Maneuvering

Triakis semifasciata, *Chiloscyllium plagiosum*, and *Squalus acanthias* actively adjust the angle of their pectoral fins to maneuver vertically in the water column (Wilga and Lauder, 2000, 2001, 2004). Rising in the water column is initiated when the posterior plane of the fin is flipped downward to produce mean obtuse dorsal fin angles around 200°, while the leading edge of the fin is rotated upward relative to the flow. This downward flipping of the posterior plane of the fin increases the chord angle to +14, and as a result the shark rises in the water. In contrast, to sink in the water the posterior plane of the pectoral fin is flipped upward relative to the anterior plane, which produces a mean obtuse dorsal fin angle of 185°. At the same time, the leading edge of the fin is rotated downward relative to the flow such that the chord angle is decreased to −22°, and the shark sinks in the water.

The dihedral angle of shark pectoral fins changes significantly during vertical maneuvering in the water column (Figure 5.16). The dihedral angle increases to −35° during rising and decreases to −5° during sinking. This

may be due to a need for greater stability during sinking behavior because the heterocercal tail generates a lift force that tends to drive the head ventrally. Holding the pectoral fins at a low dihedral angle results in greater stability during sinking compared to rising. The greater negative dihedral angle increases maneuverability and allows rapid changes in body orientation during rising.

These angular adjustments of the pectoral fins are used to maneuver vertically in the water column and generate negative and positive lift forces, which then initiate changes in the angle of the body relative to the flow. As the posterior plane of the pectoral fin is flipped down to ascend, a counterclockwise vortex, indicating upward lift force generation, is produced and shed from the trailing edge of the fin and pushes the head and anterior body upward (Figure 5.17). This vortex is readily visible in the wake as it rolls off the fin and is carried downstream. The opposite flow pattern occurs when sharks initiate a sinking maneuver in the water column. A clockwise vortex, indicating downward lift force generation, is visualized in the wake of the pectoral fin as a result of the dorsal fin flip and pulls the head and anterior body of the shark downward (Figure 5.17).

Lift forces produced by altering the planar surface of the pectoral fin to rise and sink appear to be a mechanism to reorient the position of the head and anterior body for maneuvering. Changing the orientation of the head will alter the force balance on the body as a result of interaction with the oncoming flow and will induce a change in vertical forces that will move the shark up or down in the water column. Forces generated by the pectoral fins are significantly greater in magnitude during sinking than during rising. This may be due to the necessity of reorienting the body through a greater angular change to sink from the positive body tilt adopted during steady swimming. A shark must reposition the body from a positive body tilt of 8° (mean holding angle) down through the horizontal to a negative body tilt of –11° (mean sinking angle), a change of 19°. In contrast, to rise a shark simply increases the positive tilt of the body by 14° (mean rise – hold difference), which should require less force given that the oncoming flow will assist the change from a slightly tilted steady horizontal swimming position to a more inclined rising body position.

5.2.3.4 Function of the Pectoral Fins during Benthic Station-Holding

Chiloscyllium plagiosum have a benthic lifestyle and spend much of their time resting on the substrate on and around coral reefs where current flows can be strong. To maintain position on the substrate during significant current flow, these sharks shift their body posture to reduce drag (Wilga and Lauder, 2001). The sharks reorient the longitudinal axis of the body to the flow with the head pointing upstream during current flow, but they do not orient when current flow is negligible or absent. Body angle steadily decreases from 4° at 0 *l*/s to 0.6° at 1.0 *l*/s as they flatten their body against the substrate with increasing flow speed. This reduces drag in higher current flows, thereby promoting station-holding. This behavior is advantageous in fusiform benthic fishes that experience a relatively high flow regime, such as streams where salmon parr are hatched (Arnold and Webb, 1991) and inshore coral reefs where bamboo sharks dwell (Compagno, 1984).

Chiloscyllium plagiosum also reorient the pectoral fins to generate negative lift, increase friction, and oppose downstream drag during station-holding in current flow (Wilga and Lauder, 2001). They hold the pectoral fins in a concave upward orientation, similar to that in sinking, which decreases from a mean planar angle of 174° at 0 *l*/s to a mean of 165° at 1.0 *l*/s. At the same time, the chord angle steadily decreases from a mean of 2.7° at 0 *l*/s to a mean of –3.9° at 1.0 *l*/s. Flattening the body against the substrate lowers the anterior edge of the fin, whereas elevating the posterior edge of the fin to decrease the planar angle significantly decreases the chord angle (Figure 5.18). In this orientation, water flow is deflected up and over the fin and produces a clockwise vortex that is shed from the fin tip. The clockwise vortex produces significant negative lift (mean –0.084 N) directed toward the substrate that is eight times greater than that generated during sinking. As the clockwise vortex shed from the fin rotates just behind the fin, flow recirculates upstream and pushes against the posterior surface of the fin, which opposes downstream drag. These movements generate negative lift that is directed toward the substrate and acts to increase total downward force and friction force, thereby promoting station-holding as predicted by previous studies (Arnold and Web, 1991; Webb and Gerstner, 1996), as well as a novel mechanism leading to vortex shedding that opposes downstream drag to further aid benthic station-holding (Wilga and Lauder, 2001).

5.2.3.5 Motor Activity in the Pectoral Fins

Movement of the posterior plane of the pectoral fin during sinking and rising is actively controlled by *Triakis semifasciata*. At the beginning of a rise, the pectoral fin depressors (ventral fin muscles, adductors) are active to depress the posterior portion of the pectoral fin (Figure 5.19). Small bursts of activity in the lateral hypaxialis, protractor, and levator muscles are sometimes present during rising, probably to stabilize pectoral fin position. In contrast, the pectoral fin levators (dorsal fin muscles, adductors), as well as the cucullaris and ventral hypaxialis, are strongly active during elevation of the posterior

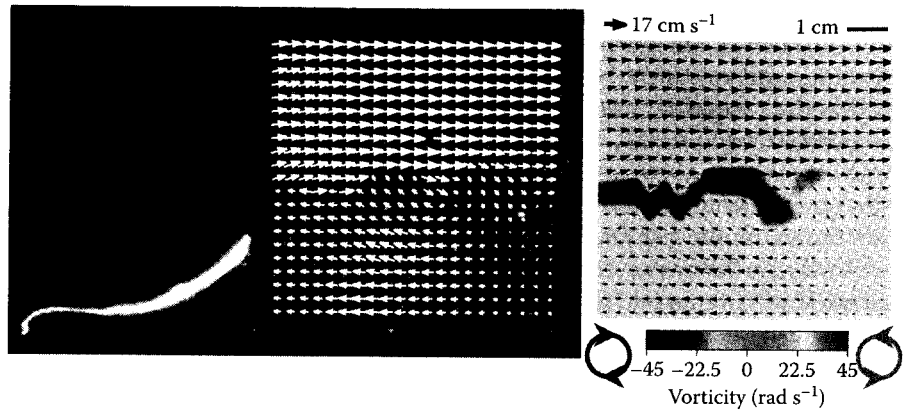

FIGURE 5.18
DPIV data from the pectoral fins of a representative bamboo shark, *Chiloscyllium plagiosum*, while station-holding on the substrate. The video image on the left shows a shark with the left pectoral fin located in the anterior end of the laser light sheet; other conventions are as in Figures 5.8 and 5.15. Note that the fin is held at a negative chord angle to the flow. A clockwise vortex (negative vorticity) was produced in the wake of the pectoral fins, which continued to rotate just behind the fin for several seconds until it was carried downstream by the flow (as seen here), after which a new vortex forms in the wake of the fin. (Adapted from Wilga, C.D. and Lauder, G.V., *J. Morphol.*, 249, 195–209, 2001.)

portion of the fin at the beginning of sinking behavior. Virtually no motor activity is present in the pectoral fin muscles while holding position at 0.5 and 1.0 *l*/s, indicating that the pectoral fins are not actively held in any particular position during steady horizontal locomotion. At higher flow speeds (1.5 *l*/s), however, recruitment of epaxial and hypaxial muscles occurs with slight activity in the pectoral fin muscles that may function to maintain stability.

Epaxial or hypaxial muscles are recruited to elevate or depress the head and anterior body during rising or sinking, respectively. At the initiation of rising behavior, simultaneously with the head pitching upward, a strong burst of activity occurs in the cranial epaxialis, while it is virtually silent during holding and sinking. Similarly, a strong burst of activity occurs in the ventral hypaxialis

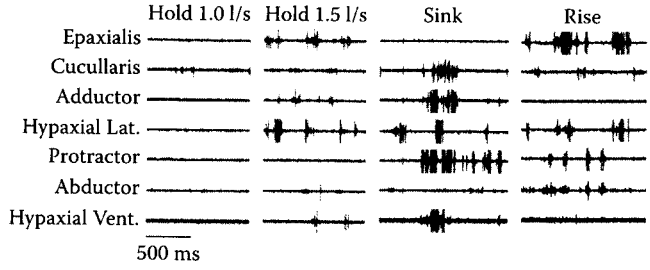

FIGURE 5.19
Electromyographic data from selected pectoral fin and body muscles during locomotion in *Triakis semifasciata* at 1.0 *l*/s for four behaviors: holding position at 1.0 and 1.5 *l*/s and sinking and rising at 1.0 *l*/s. Note the near absence of fin muscle activity while holding position at 1.0 *l*/s and recruitment of body and fin muscles at 1.5 *l*/s. The hypaxialis was implanted in both lateral (mid-lateral dorsal and posterior to pectoral fin base) and ventral (posterior to coracoid bar) positions. All panels are from the same individual. Scale bar represents 500 ms.

during the initiation of sinking behavior, again with virtually no activity during holding and rising. This shows that the head is actively elevated or depressed to rise or sink, respectively, and that conformational changes in the anterior body assist the forces generated by the pectoral fins to accomplish vertical maneuvers. Finally, antagonistic pectoral fin muscles become active as rising or sinking slows or during braking (i.e., the levators are active as rising stops and the depressors are active as sinking stops).

5.2.4 Routine Maneuvers and Escape Responses

Less well studied than steady swimming, routine maneuvers and escape responses have recently become the focus of several shark locomotion studies. Foraging turn kinematics have been analyzed in juveniles of three species: *Sphyrna tiburo*, *Sphyrna lewini*, and *Carcharhinus plumbeus* (Kajiura et al., 2003). Scalloped hammerhead sharks, *Sphyrna lewini*, are more maneuverable than sandbar sharks, *Carcharhinus plumbeus*, based on variables such as turning radius, velocity, and banking (Kajiura et al., 2003). Hammerheads do not roll the body during turns, thus rejecting the hypothesis that the cephalofoil functions as a steering wing. The cephalofoil might still have hydrodynamic functions by providing stability during maneuvers (Kajiura et al., 2003). Further investigation with larger individuals and flow visualization techniques would clarify cephalofoil function. Compared to sandbar sharks, hammerhead sharks have greater lateral flexure. This may be due to a smaller second moment of area in hammerhead sharks, which is related to cross-sectional shape of vertebrae, rather than vertebral count (Kajiura et al., 2003).

Body curvature has been assessed in shark species during routine maneuvers to determine which features of axial morphology are good predictors of maneuverability (Porter et al., 2009). The species studied were *Triakis semifasciata, Heterodontus francisci, Chiloscyllium plagiosum, Chiloscyllium punctatum,* and *Hemiscyllium ocellatum*. The best predictor of body curvature is the second moment of area of the vertebral centrum, followed by length and transverse height of vertebral centra. Body total length, fineness ratio, and width also appear to influence maneuverability (Porter et al., 2009).

Another important behavior in terms of selective pressure is escape behavior, which enables individuals to elude predators. Escape behaviors in sharks have been poorly studied, and only one study has been published to date (Domenici et al., 2004). Spiny dogfish perform C-start escape responses, which are characterized by an initial bend of the body into a "C" shape in stage I (Domenici et al., 2004). This initial conformation allows the body to accelerate in stage II when the fish straightens by thrusting the tail back to start moving away from the stimulus (Domenici and Blake, 1997). Spiny dogfish appear to have two types of escape response resulting in a bimodal distribution in duration, velocity, and acceleration (Domenici et al., 2004). Fast and slow escape responses have maximum turning rates of 766 and 1023 deg. s^{-1} and 434 and 593 deg. s^{-1}, respectively (Figure 5.20). It appears that spiny dogfish are capable of modulating the escape response based on some perceived stimulus or have two neural circuits for escape responses. Compared to bony fishes, escape responses in spiny dogfish are relatively slow; however, turning rate and turning radius are comparable (Domenici et al., 2004).

Traditionally routine and escape maneuvers have been analyzed using 2D approaches; however, for sharks that can quickly swim in any direction, except backward (Wilga and Lauder, 2000, 2001), 3D analyses and fluid dynamics studies would enable relations of body type and maneuverability to be made with escape response behavior. For example, juvenile spiny dogfish perform vertically oriented escape responses, whereas hatchling skates move horizontally (AMRM, pers. obs.).

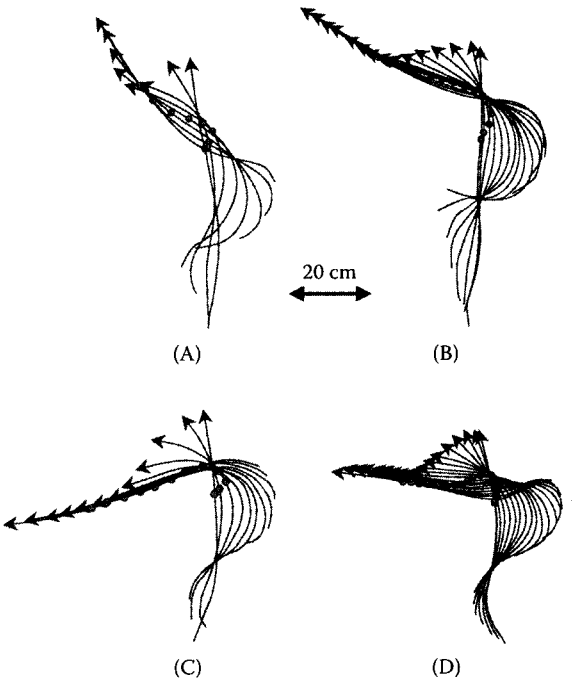

FIGURE 5.20
Midline kinematics of spiny dogfish during escape responses. Center of mass in represented in gray circles, and the head is indicated by an arrow. Consecutive lines are 40 ms apart after the onset of escape. Traces (A) and (C) are representative of fast responses; (B) and (D) represent slow responses. Note the distance covered by the center of mass in the same time for fast and slow responses (From Domenici, P. et al., *J. Exp. Biol.*, 207, 2339–2349, 2004. With permission.)

5.2.5 Synthesis

The data presented above on pectoral and caudal fin function and body orientation in the shark species studied permit construction of a new model of the overall force balance during swimming (Figure 5.21). It is useful to discuss separately the vertical force balance and the rotational (torque) balance. During steady horizontal locomotion, when sharks are holding vertical position, body weight is balanced by lift forces generated by the heterocercal tail and ventral body surface. The ventral surface generates lift both anterior and posterior to the center of body mass by virtue of its positive angle of attack to the oncoming water. Sharks adjust their body angle to modulate the total lift force produced by the body and can thus compensate for changes in body weight over both short and longer time frames.

Rotational balance is achieved by balancing the moments of forces around the center of mass. It has not been generally appreciated that the ventral body surface generates both positive and negative torques corresponding to the location of the ventral surface anterior and posterior to the center of mass. Water impacting the ventral body surface posterior to the center of mass will generate a counterclockwise torque of the same sign as that generated by the heterocercal tail. In contrast, water impacting the ventral body anterior to the center of mass will generate a clockwise torque, which is opposite in sign to that generated by the ventral body and tail posterior to the center of mass. Experimental data show that shark pectoral fins do not generate lift or torque during steady horizontal locomotion (Wilga and Lauder, 2000, 2001) as a result of their orientation relative to the flow. This stands in contrast to the textbook

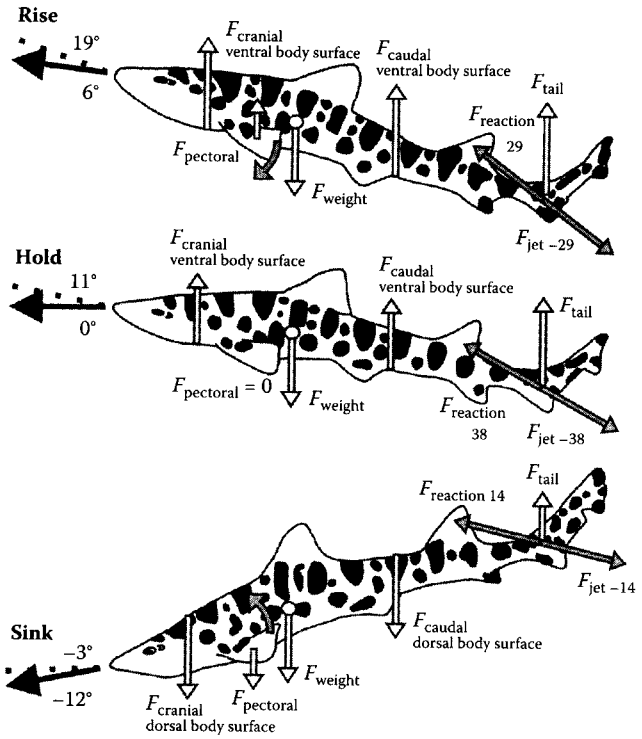

FIGURE 5.21
Schematic diagram of a force balance on swimming sharks during holding position, rising, and sinking behaviors (also representative of bamboo sharks, *Chiloscyllium punctatum*, and spiny dogfish, *Squalus acanthias*). The white circle represents the center of mass and vectors indicate forces *F* exerted by the fish on the fluid. Lift forces are generated by the ventral body surface, both anterior and posterior to the center of mass. The jet produced by the beating of the tail maintains a constant angle relative to body angle and path angle and results in an anterodorsally directed reaction force oriented dorsal to the center of mass during all three behaviors, supporting the classical model. Tail vortex jet angles are predicted means. (From Wilga, C.D. and Lauder, G.V., *J. Exp. Biol.*, 205, 2365–2374, 2002. With permission.)

depiction of shark locomotion in which the pectoral fins play a central role in controlling body position during horizontal locomotion. In our view, experimental kinematic and hydrodynamic data obtained over the last 10 years on benthic and benthopelagic species demonstrate that control of body orientation is the key to modulating lift and torques during horizontal swimming, and the pectoral fins are not used for balancing forces during horizontal swimming.

During maneuvering, however, the pectoral fins do play a key role in generating both positive and negative lift forces and hence torques about the center of mass (Figure 5.21). To rise in the water, sharks rapidly move the trailing pectoral fin edge ventrally, and a large vortex is shed, generating a corresponding lift force. This force has a clockwise rotational moment about the center of mass pitching the body up, thus increasing the angle of the body and hence the overall lift force. As a result, sharks move vertically in the water even while maintaining horizontal position via increased thrust produced by the body and caudal fin.

To stop this vertical motion or to maneuver down (sink) in the water, the trailing pectoral fin edge is rapidly elevated and sheds a large vortex, which produces a large negative lift force (Figure 5.21). This generates a counterclockwise torque about the center of mass, pitching the body down, exposing the dorsal surface to incident flow, and producing a net sinking motion. Pectoral fins thus modulate body pitch.

Overall, the force balance on swimming sharks is maintained and adjusted by small alterations in body angle and this in turn is achieved by elevation and depression of the pectoral fins. Pectoral fins thus play a critical role in shark locomotion by controlling body position and facilitating maneuvering, but they do not function to balance tail lift forces during steady horizontal locomotion.

5.3 Locomotion in Skates and Rays

Most batoids either undulate or oscillate the pectoral fins to move through the water (Figure 5.22). Basal batoids, such as guitarfishes, sawfishes, and electric rays, locomote by undulating their relatively thick tails similar to those of laterally undulating sharks (Rosenberger, 2001). Interestingly, *Rhinobatos lentiginosus*, which has a sharklike trunk and tail like all guitarfishes, also adopts a positive body angle to the flow during steady horizontal swimming (Rosenberger, 2001). Sawfishes and most electric rays are strict axial undulators and use only the tail for locomotion, whereas guitarfishes and some electric rays may supplement axial locomotion with undulations of the pectoral fin (Rosenberger, 2001). Most rays use strict pectoral fin locomotion; however, some rays, such as *Rhinoptera* and *Gymnura*, fly through the water by oscillating the pectoral fins in broad up and down strokes in a manner that would provide vertical lift similar to that of aerial bird flight (Rosenberger, 2001). Although skates undulate the pectoral fins to swim when in the water column, they have enlarged muscular appendages on the pelvic fins that are modified for walking or "punting" off the substrate (Koester and Spirito, 1999) in a novel locomotor mechanism. Although they lack the modified pelvic appendages of skates, some rays with similar habitats and prey also use punting locomotion (Macesic and Kajiura, 2010). Punting kinematics were similar across one skate and three ray species (*Raja eglanteria, Narcine brasiliensis, Urobatis jamaicensis*, and *Dasyatis sabina*), with protraction of the

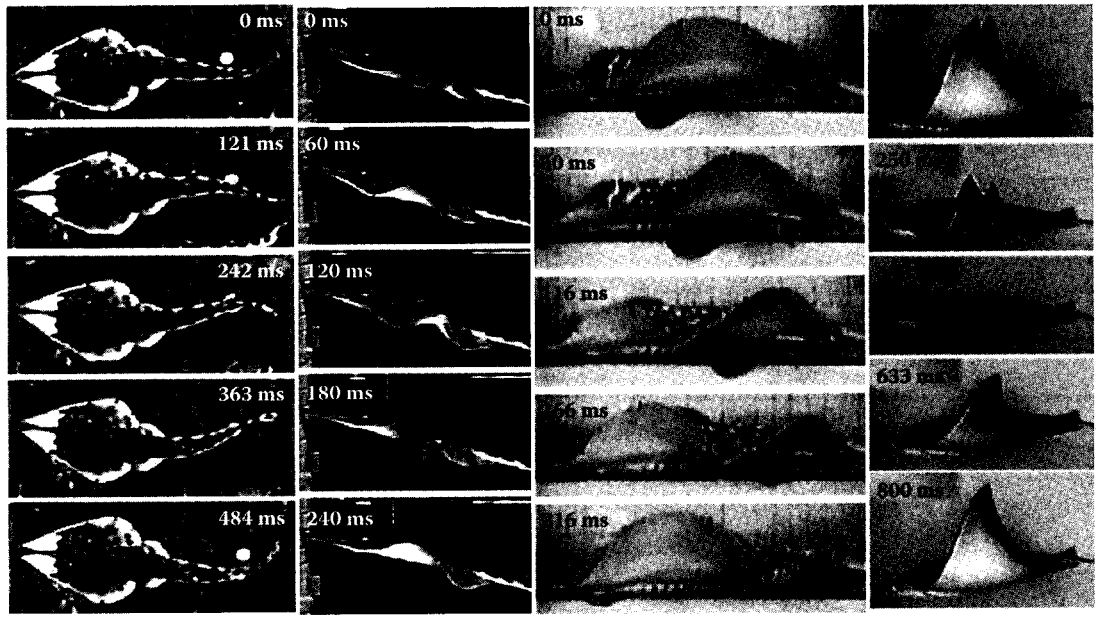

FIGURE 5.22
Successive dorsal video images of Atlantic guitarfish (*Rhinobatos lentiginosus*, left) and lateral video images of *R. lentiginosus* (second from left), blue-spotted stingray (*Taeniuralymma*, second from right), and cownose rays (*Rhinoptera bonasus*, right) swimming in a flow tank. Like sharks, *Rhinobatos lentiginosus* swims primarily with its thick shark-like tail. (From Rosenberger, L.J. and Westneat, M.W., *J. Exp. Biol.*, 202, 3523–3539, 1999; Rosenberger, L.J., *J. Exp. Biol.*, 204, 379–394, 2001. With permission.)

anterior edge of the pelvic fins followed by contact with the substrate and then retraction to push off (Macesic and Kajiura, 2010). *Raja eglanteria* and *N. brasiliensis* are true punters in which the pelvic fins are used to punt while pectorals are held horizontally. In contrast, *U. jamaicensis* and *D. sabina* augment punting by undulations of the pectoral fins, although this does not increase performance as measured by the distance traveled during a punting cycle. The musculature of true punters is highly specialized with robust crura, mobile distal joints, and specialized propterygium levators, depressors, and protractors originating from lateral processes on the pelvic girdle (Figure 5.23) (Macesic and Kajiura, 2010). In contrast, augmented punters have only one levator and depressor muscle controlling the propterygium with a reduced pelvic girdle that limits movements (Macesic and Kajiura, 2010).

Some rays are able to vary the mechanics of the pectoral fins during locomotion (Rosenberger, 2001). There appears to be a trade-off between the amplitude of undulatory waves and fin beat frequency: Those that have higher wave amplitudes have fewer waves and *vice versa* (Rosenberger, 2001). This phenomenon appears to be correlated with lifestyle. Fully benthic rays and skates that are mostly sedentary, such as *Dasyatis sabina* and *D. say*, have low-amplitude waves with high fin beat frequencies, permitting high maneuverability at low speeds, which is more suited for swimming slowly along the substrate to locate food items (Rosenberger, 2001). Fully pelagic rays are able to take advantage of the 3D environment of the water column and oscillate the pectoral fins using high-amplitude waves and low fin beat frequencies (Rosenberger, 2001). Rays and skates that have both benthic and pelagic lifestyles, such as *Raja* sp. and *Dasyatis americana*, are typically more active and have intermediate values of amplitude and frequency (Rosenberger, 2001).

Oscillatory appendage propulsors that feed on benthic mollusks and crustaceans, such as cownose and butterfly rays, do not extend the fins below the ventral body axis during swimming, presumably so they can use the lateral line canals to detect prey and also to avoid contact with the substrate (Rosenberger, 2001). In contrast, oscillatory appendage propulsors that feed in the water column (i.e., filter feeders such as manta and mobulid rays) extend the pectoral fins equally above and below the body axis during swimming (Rosenberger, 2001). Some batoids are capable of modifying the swimming mechanism dependent on habitat; *Gymnura* undulates the pectoral fins when swimming along a substrate and oscillates them when swimming in the water column (Rosenberger, 2001). Undulatory mechanisms are efficient at slow speeds, offer reduced body and fin drag, and are highly maneuverable (Blake, 1983a,b; Lighthill and Blake, 1990; Rosenberger, 2001; Walker and Westneat, 2000). In contrast, oscillatory mechanisms are efficient at fast cruising and generate greater lift but are less well suited for maneuvering

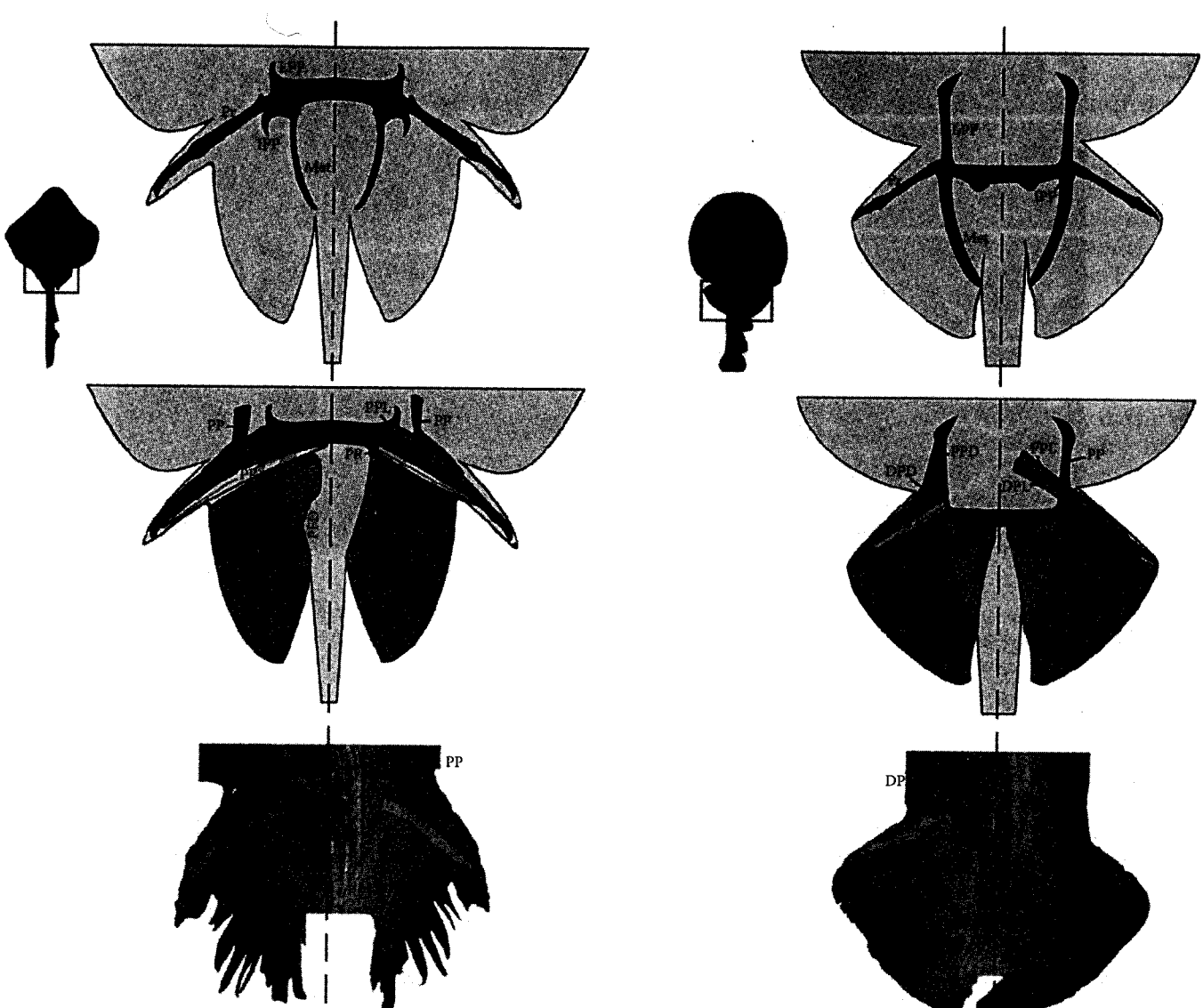

FIGURE 5.23
Schematic representation (top) and photographs (bottom) of pelvic fin skeletal elements and musculature of two benthic true punters: (A) *Raja eglanteria*, and (B) *Narcine brasiliensis*. Skeletal elements are shown in the top and middle illustrations: puboischiac bar (PB), iliac pelvic process (IPL), lateral pelvic process (LPP), metapterygium (Met), and propterygium (Pr). Pelvic musculature is shown at the middle and bottom illustrations: proximal fin depressor (PDF), distal fin depressor (DFP), distal propterygium depressor (DPD), proximal propterygium depressor (PPD), proximal fin levator (PFL), distal fin levator (DFL), proximal propterygium levator (PPL), and distal propterygium levator (DPL). The propterygium retractors (PR) and protractors (PP) were found on both dorsal and ventral sides (PP is occluded from view in the dorsal photograph of *N. brasiliensis*). Note the specializations in propterygium depressors and levators. (From Macesic, L.J. and Kajiura, S.M., *J. Morphol.*, 271, 1219–1228, 2010. With permission.)

(Blake, 1983b; Cheng and Zhaung, 1991; Chopra, 1974; Rosenberger, 2001). A recent study suggested that sensory coverage area is inversely related to the proportion of the wing used for propulsion in batoids (Jordan, 2008). However, *Myliobatis californica*, which uses oscillatory propulsion and thus is expected to have a smaller sensory area, has extensions of the lateral line and electrosensory systems along the anterior edge of the pectoral fins (Jordan, 2008).

Different strategies are employed to increase swimming speed in various batoid species (Rosenberger, 2001). Most *Dasyatis* species increase fin beat frequency, wave

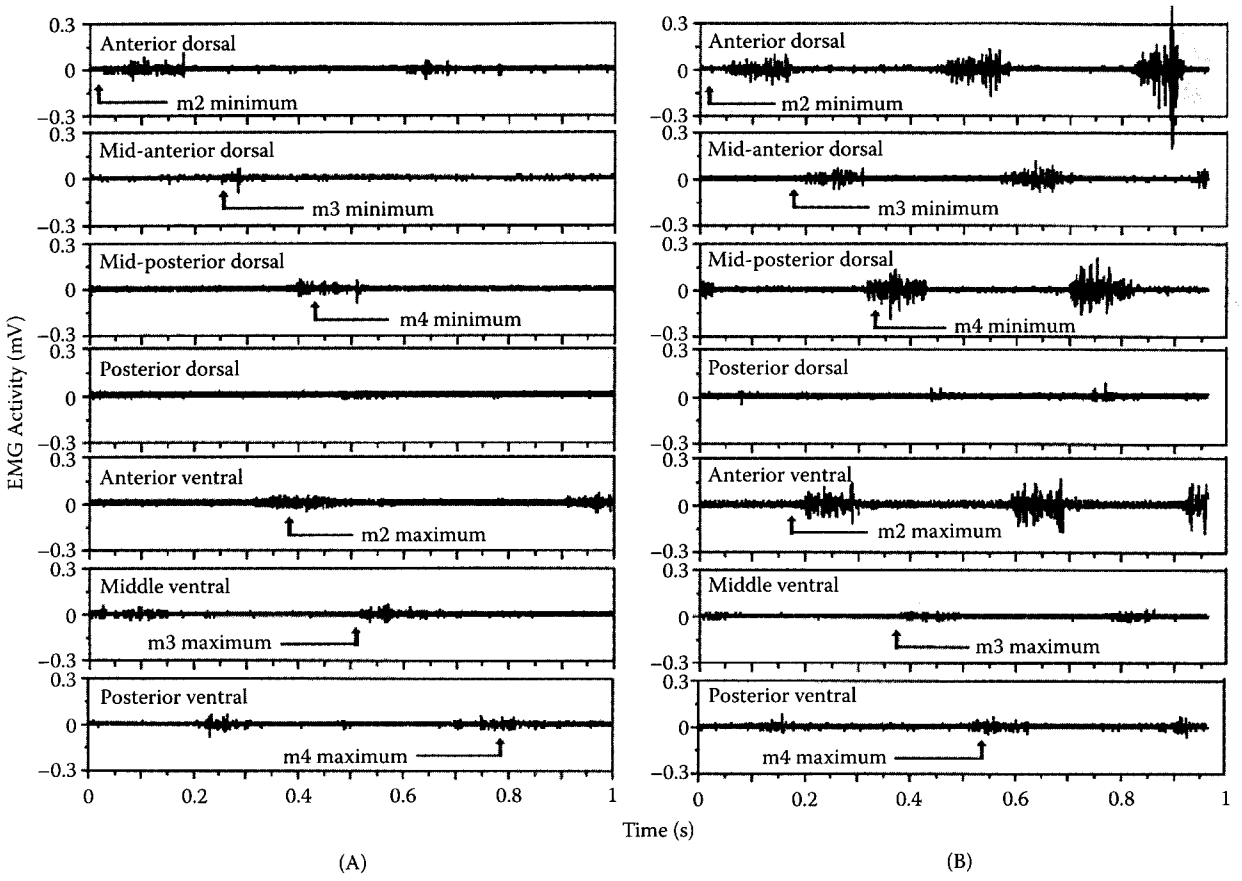

FIGURE 5.24
Electromyographic (EMG) data illustrating the muscle activity for the pectoral fin undulation of blue-spotted stingrays, *Taeniura lymma*, at a low speed of 1.2 disk length/s (A) and at a higher speed of 3.0 disk length/s (B). The electrode recordings are taken from the following muscles: anterior dorsal, mid-anterior dorsal, mid-posterior dorsal, posterior dorsal, anterior ventral, middle ventral, and posterior ventral. The arrows below the EMG activity indicate the point during the fin-beat cycle at which the anterior, middle, and posterior fin markers are at their maximum (peak upstroke) and minimum (peak downstroke) excursion. (From Rosenberger, L.J. and Westneat, M.W., *J. Exp. Biol.*, 202, 3523–3539, 1999; Rosenberger, L.J., *J. Exp. Biol.*, 204, 379–394, 2001. With permission.)

speed, and stride length to increase swimming speed while amplitude is held constant; however, *Taeniura lymma* and *D. americana* increase fin beat frequency and wave speed but decrease wave number while holding amplitude constant to increase speed (Rosenberger, 2001; Rosenberger and Westneat, 1999). Similarly, *Raja eglanteria* increases wave speed and decreases wave number to swim faster (Rosenberger, 2001; Rosenberger and Westneat, 1999). Oscillatory propulsors, such as *Rhinoptera* and *Gymnura*, increase wave speed in addition to fin-tip velocity to increase swimming speed (Rosenberger, 2001; Rosenberger and Westneat, 1999). Interestingly, *Gymnura* pauses between each fin beat at high flow speeds, similar to the burst and glide flight mechanisms of aerial birds (Rosenberger, 2001; Rosenberger and Westneat, 1999).

As expected, the dorsal and ventral fin muscles are alternately active during undulation of the pectoral fin from anterior to posterior (Figure 5.24) (Rosenberger and Westneat, 1999). The intensity of muscle contraction is increased to swim faster in *Taeniura lymma*, and the ventral muscles are also active longer than the respective dorsal muscles, indicating that the downstroke is the major power-producing stroke (Rosenberger and Westneat, 1999). Chondrichthyans are negatively buoyant; thus, lift must be generated to counter the weight of the fish as well as for locomotion. Interburst duration is decreased in *T. lymma* at higher swimming speeds with the fin muscles firing closer together (Rosenberger and Westneat, 1999).

5.4 Locomotion in Holocephalans

Chimaeras have large flexible pectoral fins that have been described as both undulatory and oscillatory. The leading edge of the pectoral fin is flapped, which then passes an undulatory wave down the pectoral fin to the

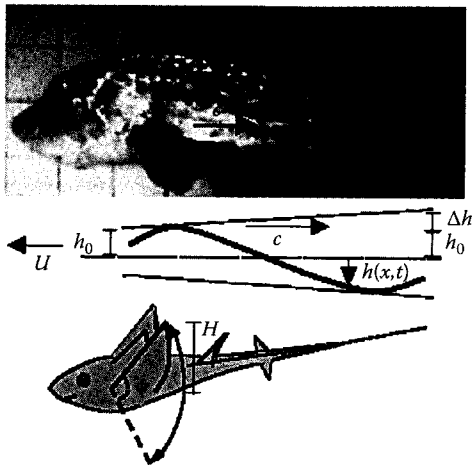

FIGURE 5.25
(Top) A ratfish with a wave (highlighted) traveling backward on its pectoral fin at wave speed c. (Middle) A two-dimensional strip oscillating with amplitude h_0 and moving forward at velocity U while a wave passes rearward at velocity c. The amplitude changes from the leading to the trailing edge by a factor ε, the ratio of Δh to h_0. The instantaneous location of a point (x) on the strip is described by $h(x,t)$, where t is time. (Bottom) Diagram of a ratfish illustrating the angle (φ) subtended by a flapping fin and tip amplitude (H). (From Combes, S.A. and Daniel, T.L., *J. Exp. Biol.*, 204, 2073–2085, 2001. With permission.)

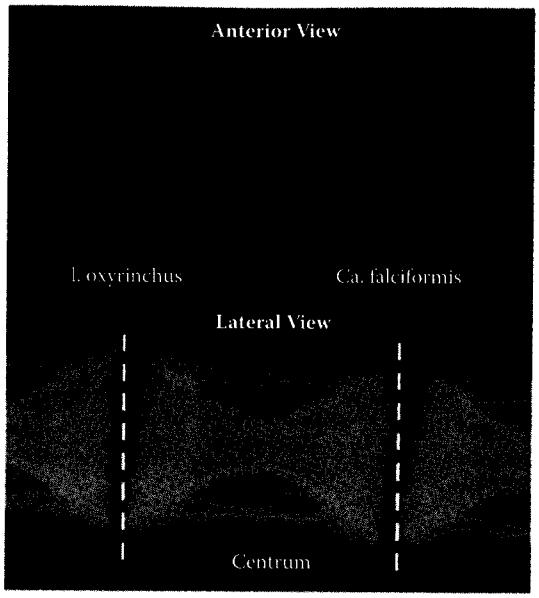

FIGURE 5.26
Radiograph of an anterior view of a mako shark (*Isurus oxyrinchus*) and silky shark (*Carcharhinus falciformis*) vertebral centra with excised neural and hemal arches. Lateral view of gulper shark (*Centrophorus granulosus*) vertebrae. (From Porter, M.E. et al., *J. Exp. Biol.*, 209, 2920–2928, 2006. With permission.)

trailing edge (Figure 5.25) (Combes and Daniel, 2001). As expected, adult chimaeras had a larger amplitude wave that was generated at a lower frequency than juvenile chimaeras (Combes and Daniel, 2001). Interestingly, there is no net chordwise bend in the pectoral fin, which averages a 0° angle of attack to the flow over a stroke cycle (Combes and Daniel, 2001). Potential flow models, based on kinematic and morphological variables measured on the chimaeras, for realistic flexible fins and theoretical stiff fins emphasize the importance of considering flexion in models of animal locomotion; significantly higher values for thrust were calculated when the fin was assumed to be stiff rather than flexible as in reality (Combes and Daniel, 2001). As predicted by the high degree of motion in the pectoral fins of white-spotted ratfish, *Hydrolagus colliei*, muscle mass corrected for body mass and the proportion of muscle inserting into the fin is greater in ratfish than spiny dogfish (Foster and Higham, 2010).

5.5 Material Properties of Chondrichthyan Locomotor Structures

Recent studies on the material properties of skeletal elements in elasmobranchs has focused on understanding the biomechanics of cartilaginous structures during locomotion (Dean and Summers, 2006; Dean et al., 2009; Porter and Long, 2010; Porter et al., 2006, 2007; Schaeffer and Summers, 2005). Material property studies of head structures indicate that tendon and cartilage experience high mechanical stresses during feeding, which is supported by theoretical studies calculating the feeding forces generated (Summers and Koob, 2002; Summers et al., 2003).

Evolution of the vertebral column and myomeres allowed the strong compressions needed to undulate the body through a dense medium such as water (Liem et al., 2001). The vertebral column is composed of multiple vertebrae, each with a central body and dorsal neural and ventral hemal arches. Figure 5.26 presents radiographs of vertebral centra. Unlike cartilage in the remaining skeletal structures of the body in living elasmobranchs that are tessellated, vertebral centra are formed by areolar calcification (Dean and Summers, 2006). Material testing revealed that vertebral centra have stiffness and strength of the same order of magnitude as mammalian trabecular bone (Porter et al., 2006). Swimming speed appears to be a good predictor of vertebral cartilage stiffness and strength in elasmobranchs. In addition, chemical composition of vertebral centra is correlated with collagen content and material stiffness and strength, except for proteoglycan content (Figure 5.27) (Porter et al., 2006). In a separate study, vertebrae were tested under compressive loads with neural arches attached or removed; failure was seen in the vertebral centra but not in the neural arches. Thus, vertebral centra are likely the main load-bearing structures of the vertebral column in sharks during routine swimming (Porter and Long, 2010).

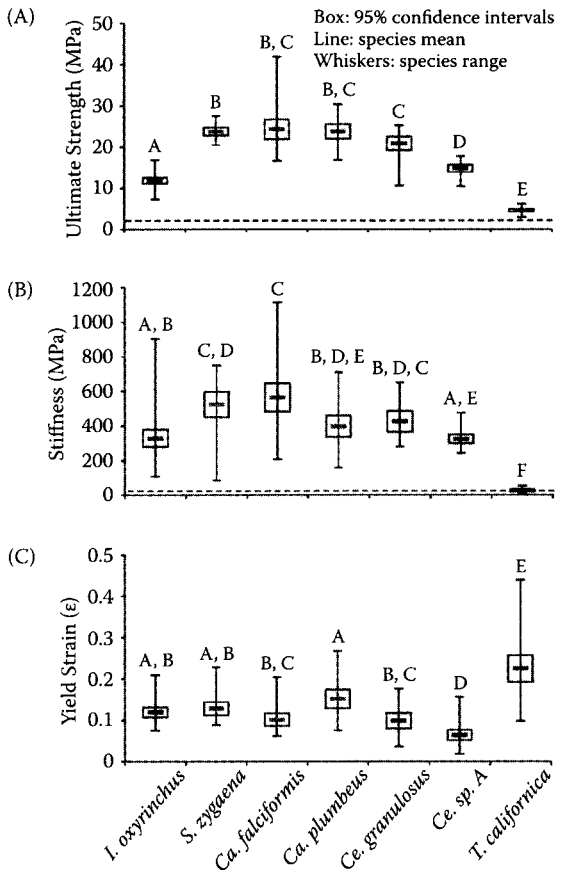

FIGURE 5.27
Material properties of mineralized cartilage in shark vertebral centra. (A) Ultimate strength (MPa) of vertebral cartilages from seven elasmobranch species showing significant differences ($F_{6,151}$ = 182.8, P < 0.001). The broken horizontal line represents the lower limits of trabecular bone. Letters above the box and whisker plot denote significant differences between species. (B) Material stiffness was significantly different among the species ($F_{6,151}$ = 54.4, P < 0.001). *Torpedo californica*, the only batoid, was less stiff than all shark species (P < 0.001). The horizontal line shows the lower limits of stiffness for trabecular bone. (C) Yield strain was significantly different among the species ($F_{6,147}$ = 27.6, P < 0.001). *T. californica* had the greatest yield strain of all species (P < 0.007). (From Porter, M.E. et al., *J. Exp. Biol.*, 209, 2920–2928, 2006. With permission.)

Locomotor mode is also a good predictor of batoid wing skeletal morphology, indicating a role of flexural stiffness (Schaeffer and Summers, 2005). Undulatory swimmers such as *Dasyatis* have chain-like catenated calcification patterns with staggered joints in the radials; oscillatory swimmers have radials completely covered with mineralization in a crustal calcification pattern. Some oscillatory species also had cross-bracing between adjacent radials that is thought to increase fin stiffness. Theoretical stiffness of fin morphology agreed with observed stiffness (Schaeffer and Summers, 2005). These studies provide further evidence of the role of material properties in determining the function and evolution of skeletal elements and locomotor modes in Chondrichthyans.

5.6 Future Directions

The diversity of shark species for which we have even basic functional data on locomotor mechanics is extremely limited. Most papers to date have focused on leopard (*Triakis*), spiny dogfish (*Squalus*), and bamboo (*Chiloscyllium*) sharks swimming under controlled laboratory conditions. A high priority for future studies of locomotion in sharks, skates, and rays is to expand the diversity of taxa studied, especially for analyses of shark mechanics. The data obtained by Rosenberger (2001) on batoid locomotion are exemplary for their broadly comparative character, but studies like this are rare, perhaps necessarily so when detailed functional data must be obtained for a variety of behaviors.

Experimental studies of kinematics and hydrodynamics would benefit from increased spatial and temporal resolution so that a more detailed picture could be obtained of patterns of fin deformation and the resulting hydrodynamic wake, especially during unsteady maneuvering behaviors. New high-resolution, high-speed digital video systems will permit a new level of understanding of fin function and its impact on locomotor performance. Such increased resolution may also permit further observations of boundary layer flows in relation to surface denticle patterns to follow up on the observation by Anderson et al. (2001) that the boundary layer of *Mustelus* swimming at 0.5 *l*/s did not separate and remained attached along the length of the body. Defocusing digital particle image velocimetry (DDPIV) and stereoscopic PIV can be used to compute flow in three dimensions and offer a new avenue for comprehensive studies of fluid dynamics in the wake of swimming elasmobranchs (Gordon et al., 2002; Lauder, 2010; Raffel et al., 2007). These studies can be coupled with computational fluid dynamics (CFD) (Lauder, 2010) to investigate limitations and compare different locomotor modes, similar to what has been done for actinopterygian fishes (Tytell et al., 2010). Biorobotics and biomimetics studies that are emerging use elasmobranchs as models and have focused mainly on batoids (Clark and Smits, 2006; Gao et al., 2009; Xu et al., 2007; Yang et al., 2009; Zhou and Low, 2010). Biorobotics offers a way to test scenarios that are not possible with living animals, such as altering Reynolds and Strouhal numbers, aspect ratios, and material properties (Clark and Smits, 2006; Lauder, 2010). Biomimetics has great potential to advance the field through the demand for detailed kinematics, material properties, and activation patterns of elasmobranch locomotion for application purposes.

More studies on the mechanical properties of elasmobranch connective tissue elements and of the role these play in transmitting forces to hydrodynamic fin control surfaces are needed. This is a key area in which *in*

vitro studies of material properties and *in vivo* analyses of how elasmobranch connective tissues function can greatly enhance our understanding of elasmobranch locomotor mechanics.

Finally, new information on locomotor structures such as fin placement and diversity might come from advances in developmental and molecular biology methods. Shark models have been used to study the evolution of paired and median fins (Cole and Currie, 2007) as well as skeletogenesis and the early origins of bone (Eames et al., 2007). To the extent that equipment and elasmobranch behavior permits, it would be extremely valuable to have quantitative 3D field data over the natural locomotor behavioral repertoire to answer such questions as what are routine swimming speeds, what are typical vertical and lateral maneuvering velocities, and what is the natural range of body angles observed during diverse locomotor behaviors? Advances in technology, such as accelerometers, can be used in shark research and can provide great insight to natural routine locomotor behaviors (Sims, 2010). Such data would serve as a link between experimental laboratory studies of shark biomechanics and locomotor performance in nature.

Acknowledgments

Support for preparation of this paper was provided by MCTES/FCT/SFRH/BD/36852/2007 to AMRM, by NSF grant DBI 97-07846 to CDW, and grants ONR N00014-09-1-0352, ONR N00014-03-1-0897, and NSF EFRI-0938043 to GVL.

References

Affleck, R.J. (1950). Some points in the function, development, and evolution of the tail in fishes. *Proc. Zool. Soc. Lond.* 120:349–368.

Aleev, Y.G. (1969). *Function and Gross Morphology in Fish*, trans. from the Russian by M. Raveh. Keter Press, Jerusalem.

Alexander, R.M. (1965). The lift produced by the heterocercal tails of Selachii. *J. Exp. Biol.* 43:131–138.

Anderson, E.J., McGillis, W., and Grosenbaugh, M.A. (2001). The boundary layer of swimming fish. *J. Exp. Biol.* 204:81–102.

Arnold, G.P. and Webb, P.W. (1991). The role of the pectoral fins in station-holding of Atlantic salmon parr (*Salmo salar* L). *J. Exp. Biol.* 156:625–629.

Bendix-Almgreen, S.E. (1975). The paired fins and shoulder girdle in *Cladoselache*, their morphology and phyletic significance. *Colloq. Int. C.N.R.S. Paris* 218:111–123.

Bernal, D., Donley, J.M., Shadwick, R.E., and Syme, D.A. (2005). Mammal-like muscles power swimming in a cold-water shark. *Nature* 437:1349–1352.

Blake, R.W. (1983a). *Fish Locomotion.* Cambridge University Press, Cambridge.

Blake, R.W. (1983b). Median and paired fin propulsion. In: Webb, P.W. and Weihs, D. (Eds.), *Fish Biomechanics.* Praeger, New York, pp. 214–247.

Bone, Q. (1999). Muscular system: microscopical anatomy, physiology, and biochemistry of elasmobranch muscle fibers. In: Hamlett, W.C. (Ed.), *Sharks, Skates, and Rays: The Biology of Elasmobranch Fishes.* The Johns Hopkins University Press, Baltimore, MD, pp. 115–143.

Breder, C.M. (1926). The locomotion of fishes. *Zool. (N.Y.)* 4:159–256.

Carroll, R.L. (1988). *Vertebrate Paleontology and Evolution.* WH Freeman, New York.

Cheng, J. and Zhaung, L. (1991). Analysis of swimming three-dimensional waving plates. *J. Fluid Mech.* 232:341–355.

Chopra, M.G. (1974). Hydrodynamics of lunate-tail swimming propulsion. *J. Fluid Mech.* 64:375–391.

Clark, R.P. and Smits, A.J. (2006). Thrust production and wake structure of a batoid-inspired oscillating fin. *J. Fluid Mech.* 562: 415–429.

Cole, N.J. and Currie, P.D. (2007). Insights from sharks: evolutionary and developmental models of fin development. *Dev. Dynam.* 236:2421–2431.

Combes, A. and Daniel, T.L. (2001). Shape, flapping and flexion: wing and fin design for forward flight. *J. Exp. Biol.* 204:2073–2085.

Compagno, L.J.V. (1973). Interrelationships of living elasmobranchs. In: Greenwood, P.H., Miles, R.S., and Patterson, C. (Eds.), Interrelationships of fishes, *Zool. J. Linn. Soc.* 53(Suppl. 1):15–61.

Compagno, L.J.V. (1984). *Sharks of the World.* United Nations Development Program, Rome.

Compagno, L.J.V. (1988). *Sharks of the Order Carcharhiniformes.* Princeton University Press, Princeton, NJ.

Compagno, L.J.V. (1999). Endoskeleton. In: Hamlett, W.C. (Ed.), *Sharks, Skates, and Rays: The Biology of Elasmobranch Fishes.* The Johns Hopkins University Press, Baltimore, MD, pp. 69–92.

Daniel, J.F. (1922). *The Elasmobranch Fishes.* University of California Press, Berkeley.

Dean, M.N. and Summers, A.P. (2006). Mineralized cartilage in the skeleton of chondrichthyan fishes. *Zoology* 109:164–168.

Dean, M.N., Mull, C.G., Gorb, S.N., and Summers, A.P. (2009). Ontogeny of the tessellated skeleton: insight from the skeletal growth of the round stingray *Urobatis halleri*. *J. Anat.* 215:227–239.

Dickinson, M.H. (1996). Unsteady mechanisms of force generation in aquatic and aerial locomotion. *Am. Zool.* 36:537–554.

Domenici, P. and Blake, R.W. (1997). Fish fast-start kinematics and performance. *J. Exp. Biol.* 200:1165–1178.

Domenici, P., Standen, E.M., and Levine, R.P. (2004). Escape manoeuvres in the spiny dogfish (*Squalus acanthias*). *J. Exp. Biol.* 207:2339–2349.

Donley, J. and Shadwick, R. (2003). Steady swimming muscle dynamics in the leopard shark *Triakis semifasciata*. *J. Exp. Biol.* 206:1117–1126.

Donley, J.M., Shadwick, R.E., Sepulveda, C.A., Konstantinidis, P., and Gemballa, S. (2005). Patterns of red muscle strain/activation and body kinematics during steady swimming in a lamnid shark, the shortfin mako (*Isurus oxyrinchus*). *J. Exp. Biol.* 208:2377–2387.

Drucker, E.G. and Lauder, G.V. (1999). Locomotor forces on a swimming fish: three-dimensional vortex wake dynamics quantified using digital particle image velocimetry. *J. Exp. Biol.* 202:2393–2412.

Drucker, E.G. and Lauder, G.V. (2005). Locomotor function of the dorsal fin in rainbow trout: kinematic patterns and hydrodynamic forces. *J. Exp. Biol.* 208:4479–4494.

Eames, B.F., Allen, N., Young, J., Kaplan, A., Helms, J.A., and Schneider, R.A. (2007). Skeletogenesis in the swell shark *Cephaloscyllium ventriosum*. *J. Anat.* 210:542–554.

Ferry, L.A. and Lauder, G.V. (1996). Heterocercal tail function in leopard sharks: a three-dimensional kinematic analysis of two models. *J. Exp. Biol.* 199:2253–2268.

Fish, F.E. and Shannahan, L.D. (2000). The role of the pectoral fins in body trim of sharks. *J. Fish Biol.* 56:1062–1073.

Flammang, B.E. (2010). Functional morphology of the radialis muscle in shark tails. *J. Morphol.* 271:340–352.

Foster, K.L. and Higham, T.E. (2010). How to build a pectoral fin: functional morphology and steady swimming kinematics of the spotted ratfish (*Hydrolagus colliei*). *Can. J. Zool.* 88:774–780.

Gao, J., Bi, S., Li, J., and Liu, C. (2009). Design and experiments of robot fish propelled by pectoral fins. *ROBIO* 2009:445–450.

Garman, S. (1913). The Plagiostoma (sharks, skates, and rays). *Mem. Mus. Comp. Zool. Harvard Coll.* 36.

Gemballa, S., Konstantinidis, P., Donley, J.M., Sepulveda, C., and Shadwick, R.E. (2006). Evolution of high-performance swimming in sharks: transformations of the musculotendinous system from subcarangiform to thunniform swimmers. *J. Morphol.* 267:477–493.

Gordon, M.S., Hove, J.R., and Bartol, I.K. (2002). Dynamics and energetics of animal swimming and flying: introduction. *Integr. Comp. Biol.* 42:960–963.

Gray, J. (1968). *Animal Locomotion*. Weidenfeld & Nicolson, London.

Grove, A.J. and Newell, G.E. (1936). A mechanical investigation into the effectual action of the caudal fin of some aquatic chordates. *Ann. Mag. Nat. Hist.* 17:280–290.

Harris, J.E. (1936). The role of the fins in the equilibrium of the swimming fish. I. Wind tunnel tests on a model of *Mustelus canis* (Mitchell). *J. Exp. Biol.* 13:476–493.

Harris, J.E. (1953). Fin patterns and mode of life in fishes. In: Marshall, S.M. and Orr, A.P. (Eds.), *Essays in Marine Biology*. Oliver & Boyd, Edinburgh, pp. 17–28.

Jordan, L.K. (2008). Comparative morphology of stingray lateral line canal and electrosensory systems. *J. Morphol.* 269:1325–1339.

Kajiura, S.M., Forni, J.B., and Summers, A.P. (2003). Maneuvering in juvenile carcharhinid and sphyrnid sharks: the role of the hammerhead shark cephalofoil. *Zoology* 106:19–28.

Kemp, N.E. (1999). Integumentary system and teeth. In: Hamlett, W.C. (Ed.), *Sharks, Skates, and Rays: The Biology of Elasmobranch Fishes. The* Johns Hopkins University Press, Baltimore, MD, pp. 43–68.

Koester, D.M. and Spirito, C.P. (1999). Pelvic fin locomotion in the skate, *Leucoraja erinacea*. *Am. Zool.* 39:55A.

Krothapalli, A. and Lourenco, L. (1997). Visualization of velocity and vorticity fields. In: Nakayama, Y. and Tanida, Y. (Eds.), *Atlas of Visualization*, Vol. 3. CRC Press, Boca Raton, FL, pp. 69–82.

Kundu, P. (1990). *Fluid Mechanics*. Academic Press, San Diego.

Lauder, G.V. (2000). Function of the caudal fin during locomotion in fishes: kinematics, flow visualization, and evolutionary patterns. *Am. Zool.* 40:101–122.

Lauder, G.V. (2010). Swimming hydrodynamics: ten questions and the technical approaches needed to resolve them. In: Taylor, G.K., Triantafyllou, M.S., and Tropea, C. (Eds.), *Animal Locomotion*. Springer-Verlag, Berlin, pp. 3–15.

Lauder, G.V. and Drucker E. (2002). Forces, fishes, and fluids: hydrodynamic mechanisms of aquatic locomotion. *News Physiol. Sci.* 17:235–240.

Lauder, G.V. and Madden, P.G.A. (2008). Advances in comparative physiology from high-speed imaging of animal and fluid motion. *Annu. Rev. Physiol.* 70:143–163.

Lauder, G.V., Nauen, J., and Drucker, E.G. (2002). Experimental hydrodynamics and evolution: function of median fins in ray-finned fishes. *Integr. Comp. Biol.* 42:1009–1017.

Lauder, G.V., Drucker, E.G., Nauen, J., and Wilga, C.D. (2003). Experimental hydrodynamics and evolution: caudal fin locomotion in fishes. In: Bels, V., Gasc, J.P., and Casinos, A. (Eds.), *Vertebrate Biomechanics and Evolution*, Bios Scientific Publishers, Oxford, pp. 117–135.

Liao, J. and Lauder, G.V. (2000). Function of the heterocercal tail in white sturgeon: flow visualization during steady swimming and vertical maneuvering. *J. Exp. Biol.* 203:3585–3594.

Liem, K.F. and Summers, A.P. (1999). Muscular system. In: Hamlett, W.C. (Ed.), *Sharks, Skates, and Rays: The Biology of Elasmobranch Fishes*, The Johns Hopkins University Press, Baltimore, MD, pp. 93–114.

Liem, K.F., Bemis, W.E., Walker, Jr., W.F., and Grande, L. (2001). *Functional Anatomy of the Vertebrates: An Evolutionary Perspective*, 3rd ed. Harcourt, New York.

Lighthill, J. and Blake, R. (1990). Biofluid dynamics of balistiform and gymnotiform locomotion. Part 1. Biological background and analysis by elongated-body theory. *J. Fluid. Mech.* 212:183–207.

Lindsey, C.C. (1978). Form, function, and locomotory habits in fish. In: Hoar, W.S. and Randall, D.J. (Eds.), *Fish Physiology*. Vol. 7. *Locomotion*. Academic Press, New York, pp. 1–100.

Lingham-Soliar, T. (2005). Dorsal fin in the white shark, *Carcharodon carcharias*: a dynamic stabilizer for fast swimming. *J. Morphol.* 263:1–11.

Macesic, L.J. and Kajiura, S.M. (2010). Comparative punting kinematics and pelvic fin musculature of benthic batoids. *J. Morphol.* 271:1219–1228.

Magnan, A. (1929). Les charactéristiques géométriqes et physiques des poisons. *Ann. Sci. Nat. Zool.* 10:1–132.

Nauen, J.C. and Lauder, G.V. (2002). Quantification of the wake of rainbow trout (*Oncorhynchus mykiss*) using three-dimensional stereoscopic digital particle image velocimetry. *J. Exp. Biol.* 205:3271–3279.

Perry, C.N., Cartamil, D.P., Bernal, D. et al. (2007). Quantification of red myotomal muscle volume and geometry in the shortfin mako shark (*Isurus oxyrinchus*) and the salmon shark (*Lamna ditropis*) using T1-weighted magnetic resonance imaging. *J. Morphol.* 268:284–292.

Porter, M.E. and Long, Jr., J.H. (2010). Vertebrae in compression: mechanical behavior of arches and centra in the gray smooth-hound shark (*Mustelus californicus*). *J. Morphol.* 271:366–375.

Porter, M.E., Beltrán, J.L., Koob, T.J., and Summers, A.P. (2006). Material properties and biochemical composition of mineralized vertebral cartilage in seven elasmobranch species (Chondrichthyes). *J. Exp. Biol.* 209:2920–2928.

Porter, M.E., Koob, T.J., and Summers, A.P. (2007). The contribution of mineral to the material properties of vertebral cartilage from the smooth-hound shark *Mustelus californicus*. *J. Exp. Biol.* 210:3319–3327.

Porter, M.E., Roque, C.M., and Long, Jr., J.H. (2009). Turning maneuvers in sharks: predicting body curvature from axial morphology. *J. Morphol.* 270:954–965.

Pridmore, P.A. (1995). Submerged walking in the epaulette shark *Hemiscyllium ocellatum* (Hemiscyllidae) and its implications for locomotion in rhipidistian fishes and early tetrapods. *Zoology* 98:278–297.

Raffel, M., Willert, C.E., Wereley, S.T., and Kompenhans, J. (2007). *Particle Image Velocimetry: A Practical Guide*, 2nd ed. Springer, Berlin.

Reif, W.E. and Weishampel, D.B. (1986). Anatomy and mechanics of the lunate tail in lamnid sharks. *Zool. Jahrb. Anat.* 114:221–234.

Rosenberger, L. (2001). Pectoral fin locomotion in batoid fishes: undulation *versus* oscillation. *J. Exp. Biol.* 204:379–394.

Rosenberger, L.J. and Westneat, M.W. (1999). Functional morphology of undulatory pectoral fin locomotion in the stingray *Taeniura lymma* (Chondrichthyes: Dasyatidae). *J. Exp. Biol.* 202:3523–3539.

Schaeffer, J.T. and Summers, A.P. (2005). Batoid wing skeletal structure: novel morphologies, mechanical implications, and phylogenetic patterns. *J. Morphol.* 264:298–313.

Shirai, S. (1996). Phylogenetic interrelationships of neoselachians (Chondrichthyes: Euselachii). In: Stiassny, M., Parenti, L., and Johnson, G.D. (Eds.), *Interrelationships of Fishes*. Academic Press, San Diego, pp. 9–34.

Simons, J.R. (1970). The direction of the thrust produced by the heterocercal tails of two dissimilar elasmobranchs: the Port Jackson shark, *Heterodontus portusjacksoni* (Meyer), and the piked dogfish, *Squalus megalops* (Macleay). *J. Exp. Biol.* 52:95–107.

Simons, M. (1994). *Model Aircraft Aerodynamics*. Argus Books, Herts, U.K.

Sims, D.W. (2010). Tracking and analysis techniques for understanding free-ranging shark movements and behavior. In: Carrier, J.C., Musick, J.A., and Heithaus, M.R. (Eds.), *Sharks and Their Relatives II*. CRC Press, Boca Raton, FL, pp. 351–392.

Smith, H.C. (1992). *The Illustrated Guide to Aerodynamics*. TAB Books, New York.

Stamhuis, E.J. (2006). Basics and principles of particle image velocimetry (PIV) for mapping biogenic and biologically relevant flows. *Aquat. Ecol.* 40:463–479.

Standen, E.M. (2010). Muscle activity and hydrodynamic function of pelvic fins in trout (*Oncorhynchus mykiss*). *J. Exp. Biol.* 213:831–841.

Standen, E.M. and Lauder, G.V. (2005). Dorsal and anal fin function in bluegill sunfish *Lepomis macrochirus*: three-dimensional kinematics during propulsion and maneuvering. *J. Exp. Biol.* 208:2753–2763.

Standen, E.M. and Lauder, G.V. (2007). Hydrodynamic function of dorsal and anal fins in brook trout (*Salvelinus fontinalis*). *J. Exp. Biol.* 210:340–356.

Summers, A.P. and Koob, T.J. (2002). The evolution of tendon: morphology and material properties. *Comp. Biochem. Phys. A* 133:1159–1170.

Summers, A.P., Koob-Emunds, M.M., Kajiura, S.M., and Koob, T.J. (2003). A novel fibrocartilaginous tendon from an elasmobranch fish (*Rhinoptera bonasus*). *Cell Tissue Res.* 312:221–227.

Thomson, K.S. (1971). The adaptation and evolution of early fishes. *Q. Rev. Biol.* 46:139–166.

Thomson, K.S. (1976). On the heterocercal tail in sharks. *Paleobiology* 2:19–38.

Thomson, K.S. and Simanek DE. (1977). Body form and locomotion in sharks. *Am. Zool.* 17:343–354.

Tytell, E.D., Standen, E.M., and Lauder, G.V. (2008). Escaping flatland: three dimensional kinematics and hydrodynamics of median fins in fishes. *J. Exp. Biol.* 211:187–195.

Tytell, E.D., Borazjani, I., Sotiropoulos, F. et al. (2010). Disentangling the functional roles of morphology and motion in the swimming of fish. *Int. Comp. Biol.* 50:1140–1154.

Walker, J.A. and Westneat, M.W. (2000). Mechanical performance of aquatic rowing and flying. *Proc. R. Soc. Lond. B* 267:1875–1881.

Webb, P.W. (1984). Form and function in fish swimming. *Sci. Am.* 251:72–82.

Webb, P.W. (1988). Simple physical principles and vertebrate aquatic locomotion. *Am. Zool.* 28:709–725.

Webb, P.W. and Blake, R.W. (1985). Swimming. In: Hildebrand, M. et al. (Eds.), *Functional Vertebrate Morphology*. Harvard University Press, Cambridge, MA, pp. 110–128.

Webb, P.W. and Gerstner, C.L. (1996). Station-holding by the mottled sculpin, *Cottus bairdi* (Teleostei: Cottidae) and other fishes. *Copeia* 1996:488–493.

Webb, P.W. and Keyes, R.S. (1982). Swimming kinematics of sharks. *Fish Bull.* 80:803–812.

Wilga, C.D. and Lauder, G.V. (1999). Locomotion in sturgeon: function of the pectoral fins. *J. Exp. Biol.* 202:2413–2432.

Wilga, C.D. and Lauder GV. (2000). Three-dimensional kinematics and wake structure of the pectoral fins during locomotion in leopard sharks *Triakis semifasciata*. *J. Exp. Biol.* 203:2261–2278.

Wilga, C.D. and Lauder, G.V. (2001). Functional morphology of the pectoral fins in bamboo sharks, *Chiloscyllium plagiosum*: benthic versus pelagic station holding. *J. Morphol.* 249:195–209.

Wilga, C.D. and Lauder, G.V. (2002). Function of the heterocercal tail in sharks: quantitative wake dynamics during steady horizontal swimming and vertical maneuvering. *J. Exp. Biol.* 205:2365–2374.

Wilga, C.D. and Lauder, G.V. (2004). Biomechanics of locomotion in sharks, rays and chimeras. In: Carrier, J.C., Musick, J., and Heithaus, M. (Eds.), *Biology of Sharks and Their Relatives*. CRC Press: Boca Raton, FL, pp. 139–164.

Willert, C.E. and Gharib, M. (1991). Digital particle image velocimetry. *Exp. Fluids* 10:181–193.

Xu, Y., Zong, G., Bi, S., and Gao, J. (2007). Initial development of a flapping propelled unmanned underwater vehicle (UUV). *ROBIO* 2007:514–529.

Yang, S., Qiu, J., and Han, X. (2009). Kinematics modeling and experiments of pectoral oscillation propulsion robotic fish. *J. Bionic Eng.* 6:174–179.

Zangerl, R. (1973). *Interrelationships of Early Chondrichthyans*. Academic Press, London.

Zhou, C. and Low, K. (2010). Better endurance and load capacity: an improved design of Manta Ray Robot (RoMan-II). *J. Bionic Eng.* 7(Suppl.):S137–S144.